PCC Pavement Acceptance Criteria for New Construction When Built-In Curling Exists

Final Report

Submitted to
MICHIGAN DEPARTMENT OF TRANSPORTATION
Construction and Technology Division
Lansing, Michigan

by
Will Hansen (Principal Investigator)
Ya Wei (Graduate Research Assistant)

Department of Civil and Environmental Engineering
The University of Michigan
College of Engineering

Ann Arbor, MI 48109-2125

Michigan Department of Transportation
Construction and Technology Division
Research Report RC-1481

Technical Report Documentation Page

Report No: Research Report RC-1481	2. Government Accession No.	3. MDOT Project Manager: David L. Smiley
4. Title and Subtitle: PCC Pavement Acceptance Criteria for New Construction When Built-In Curling Exists		5. Report Date: February 2008
7. Author(s) Will Hansen & Ya Wei, University of Michigan		6. Performing Organization Code
9. Performing Organization Name and Address: The University of Michigan Ann Arbor, MI 48109-2125		8. Performing Org Report No.
12. Sponsoring Agency Name and Address: Michigan Department of Transportation; Construction and Technology Division; P.O. Box 30049 Lansing, MI 48909		10. Work Unit No. (TRAIS) 11. Contract Number: 2006-0412 11(a). Authorization Number: 1
15. Supplementary Notes		13. Type of Report & Period Covered 14. Sponsoring Agency Code

16. Abstract: Top-down, mid-slab cracking from built-in curling/warping is a major distress type that exists with two Michigan JPCP projects (I-94, CS 11017 and I-96, CS 47065) on unbound OGDC. A characteristic feature of this distress is its rapid initiation and development rate. Within 5 years after construction, 90% or more of slabs in the truck lane have developed full-depth cracking with associated spalling and faulting. Rehabilitation options are generally not cost effective.

This study's major objectives are two-fold:

1. Determine, from field and laboratory measurements, the magnitude of built-in curl/warp from a temperature gradient and moisture shrinkage gradient for Michigan conditions; and the resulting effect on JPCP resistance to mid-slab, top-down fatigue cracking.
2. Establish, based on these results and Finite Element analysis, critical values for built-in curl/warp to develop additional MDOT QC/QA acceptance criteria.

This research study achieved its objective of providing justification for the development of new acceptance criteria (specifications) to be used during construction for concrete pavement placement. Also, because the contractor's construction practices can have long term ramifications affecting the concrete slab's condition, continued department monitoring of its condition after construction (contract) is completed, is warranted.

A major new finding of this study is that moisture warping from exposure to water at the slab bottom causes permanent slab joint/corner uplift resulting in fatigue cracking from truck loading at these unsupported joints.

The findings support MDOT adopts a field surface profile procedure for monitoring the severity of slab uplift to foresee the possibility of top-down cracking forming. The profiling process can also be the basis of additional QC/QA specifications.

17. Key Words Acceptance criteria, built-in curl/warp, surface profiling, top-down cracking, test methods,	18. Distribution Statement No restrictions. This document is available to the public through the Michigan Department of Transportation.		
19. Security Classification (report) Unclassified	20. Security Classification (Page) Unclassified	21. No of Pages	22. Price

PCC Pavement Acceptance Criteria for New Construction When Built-In Curling Exists

Final Report

Submitted to
MICHIGAN DEPARTMENT OF TRANSPORTATION
Construction and Technology Division
Lansing, Michigan

by
Will Hansen (Principal Investigator)
Ya Wei (Graduate Research Assistant)

Department of Civil & Environmental Engineering
University of Michigan
2350 Hayward
Ann Arbor, MI 48109-2125

DISCLAIMER

The contents of this report reflect the views of the author/principal investigator who is responsible for the facts and the accuracy of the data presented herein. The contents do not necessarily reflect the views or policies of the Michigan Department of Transportation or the Federal Highway Administration. This report does not constitute a standard, specification, or regulation.

ACKNOWLEDGEMENTS

The authors would like to thank Michigan Department of Transportation (MDOT) for sponsoring the project "PCC Pavement Acceptance Criteria for New Construction when Built-in Curling Exists", UM project number F009839-047121. The authors thank Tim Stallard, MDOT, for assistance in the field instrumentation, Kurt Bancroft for assistance in FWD testing and Andy Bennett, MDOT, for assisting the team in field work. The authors would also like to thank Dave Smiley who served as project manager for MDOT during the second and third year of this project. His suggestions and guidance throughout were greatly appreciated.

TABLE OF CONTENTS

LIST OF TABLES

LIST OF FIGURES

Executive Summary

Project Background

Recently completed research (Hansen et al. 2007) by the University of Michigan has shown that mid-slab cracking of jointed plain concrete pavement (JPCP) on unbound OGDC is dependent upon several factors. A primary factor is whether the underlying base stays in full contact with the slab. The reference study found several instances of a loss of slab support after construction. This phenomenon is also occurring nationally (Beckemeyer et al., 2002, Rao and Roesler, 2005) and internationally (Poblete et al., 1990, Springenschmid and Plannerer, 2001). The recent study by Beckemeyer et al. found that slab uplift was due to thermal and moisture effects. These factors are also suspected to exist for the I-94, CS 11017, and I-96, CS 47065, projects that developed rapid top-down mid-slab cracking soon after construction.

Project Major Objectives

This study was initiated in December 2003 with the following major objectives:

- Determine the magnitude of built-in curl from a temperature gradient at time of final set.
- Determine daily and seasonal temperature gradients for Michigan seasonal conditions.
- Determine the contribution to slab uplift from moisture warping.
- Develop a field test method to be used as the basis for a new acceptance criterion by MDOT to quantify the severity of slab uplift during and after construction.

Study Approach

Built-in construction curl (i.e. temperature difference between top and bottom at time of final set) was obtained from field instrumented slabs. One project, I-94 Demo Project, CS 82022, was instrumented with wireless sensors during summer-time construction, June 7, 2005. The other project located on US 23, CS 25031, Flint, was instrumented in late fall, October 27, 2005. The respective slab temperature differences are shown in Figure 2-2.

The influence of moisture warping on slab uplift was determined from laboratory beam tests.

Surface profile measurements were obtained for the I-96 JPCP project, CS 47065, during the summer of 2005, which had developed premature mid-slab cracking.

Pavement slab modeling was used to support this study's findings. The finite element program (ISLAB 2000) that is dedicated to pavement analysis was used.

Project Major Findings:

Built-in curl from construction: The built-in temperature curl is determined from the temperature difference between the slab top and bottom at final set. Rhodes, (1950), found that this value depends on several factors, such as base and air

temperature, time of day of placement, concrete initial temperature and slab thickness. These study findings agree with his results that a high of 20^0F (equivalent -20^0F) can be expected during summertime construction. This study further showed that a maximum temperature difference of -3^0F (equivalent $+3^0$F) can be expected for late fall paving, as shown in Figure 4-2 ((a) and (b)).

Daily Curl: Daily curl ranges from -10^0F at 6 am to $+15^0$F at 12 noon on clear summer days as seen in Figure 4-1.

Moisture Warping: The major factor causing slab uplift is moisture warping from continued wetting of the slab's bottom surface. Figure 3-5 shows that uplift from similar laboratory beam wetting is much larger than uplift from drying shrinkage alone.

Acceptance Criteria for Quantifying Built-in Curl/Warp: The amount of slab corner uplift was found to be a useful and practical parameter for the initial assessment of fatigue risk, as it can be monitored and measured over time. Figure 5-2 illustrates the uplift limits versus slab thickness predicted by ISLAB 2000. For example, for a 10-in.-thick slab fatigue cracking can develop if the corner uplift exceeds a range of 0.07 inch to 0.120 inch depending on whether creep effects are considered. If the uplift of a 15 ft JPCP on an OGDC base exceeds this range at any given time, fatigue is expected to initiate causing partial-depth cracking at the outer edge at mid-slab, where combined slab stresses are greatest.

Case Study: The results developed from finite element analysis were substantiated from a project example/case study. Surface elevation measurements along the outer edge, lane marking of west bound, were taken on warm sunny days during June and July 2005. Slabs were found to be in a permanent upward-concave condition for a series of visibly crack-free slabs, as seen from Figure 5-3. The uplift ranged from 0.08 – 0.20 inch, well within the predicted range to initiate fatigue cracking.

Project recommendation and needs for implementation of project findings: The results of this study suggest that poor subsurface drainage is the major cause for the permanent joint uplift condition for I-96 JPCP project CS 47065. There are also possible design and construction issues related to the JPCP drainage system, such as type of drainage layers (dense-graded separator layer versus geotextile membrane) and location of the underdrain, that need investigation. Portions of the base/subbase are becoming temporarily or permanently saturated along the slab-shoulder edge leading to pumping erosion and wetting of the underlying slab surface, as water is not getting to the outlet drain trench soon enough.

Finding Implementation: The steps involved to implement the study's findings, after review and acceptance by the department, include:

- **Education** –Several new terms and concepts were introduced in this report. The department's affected technical staff will need some additional classroom

explanation of these concepts to better understand their relationships to concrete pavement performance. Additional training and usage of the Finite Element Model, ISLAB2000, is needed, which is essential for pavement analysis.

- **Communication -** The department will need to explain the need for the additional acceptance criteria to the construction industry through their in-place committee contacts.

- **Preparation/Development -** The department will need to draft and implement several new procedures, especially those involving quality control. These will include:

    - A testing procedure, similar to UM's for beam uplift measuring the warping potential of various concrete mixtures.
    - Temperature monitoring of the concrete slab during hot weather paving to determine its temperature gradient at time of set in order to calculate the extent and severity of built-in construction curl that may have occurred. Temperature monitoring should continue after construction to determine average daily temperature fluctuations through the slab.
    - A procedure, like used in the study, for determining the slab's surface profile to quantify any corner uplift and its duration. Monitoring should continue long term, as slab uplift caused by moisture warping only develops if subsurface water becomes trapped and remains in contact with the slab bottom.

- **Introduction of New Test Procedures -** The department should select one or more pavement projects to implement and demonstrate the new specification requirements. The projects would provide the necessary adjustment time before the requirements are made permanent.

1. BACKGROUND/INTRODUCTION

1.1 Background

Recently completed research (Hansen et al. 2007) by the University of Michigan involving the causes of mid-slab cracking of jointed plain concrete pavement (JPCP) has found that the occurrence of cracking is dependent upon several factors. A primary factor is whether the underlying base remains in full contact with the slab. The reference study found several instances of loss of support. It also noted that this phenomenon is also occurring nationally (Beckemeyer et al., 2002). The Beckemeyer study found that loss of support was primarily due to slab uplift associated with permanent curl/warp condition. The causes were thermal and moisture shrinkage. These factors are suspected to exist for the 1997 JPCP on I-96, CS 47065, in Livingston Co.

This study was initiated in December 2003 to validate causes for the occurring loss of support and suggest acceptance criteria to mitigate this phenomenon during construction.

1.2 Introduction

Curling and warping of a concrete slab, caused by differences in temperature and moisture, respectively, between the top and bottom slab surfaces, are deviations from its original shape. These two terms are often used interchangeably. The slab's shape is constantly adapting to the thermal gradient change within a cross section; this causes slabs to curl downward when the top surface is warmer than the bottom, while an upward curl results when the bottom of the slab is warmer than the top. Moisture warping typically results in slab corner uplift due to a moisture gradient between slab top (dry) and bottom (wet). These out of plane upward movements mean that a slab is almost never in full contact with the base/subbase.

At the time of final set the slab has a temperature gradient corresponding to a full contact area between the slab and the base. This temperature gradient determines built-in construction curl. Morning paving conditions during summer favor development of a positive temperature difference between slab top and bottom (Rhodes, 1950). As the surface cools the slab has a tendency to curl upward. Thus, a positive temperature gradient at time of set is equivalent to a built-in negative gradient of similar magnitude. In the study by Beckemeyer et al. (2002), the built-in equivalent negative temperature difference between slab top and bottom was indirectly estimated from the corner movement of actual field slabs to be between -22°F and -29°F after construction. Other studies (Franklin et al. 1969, Eisenmann et al. 1990, Poblete et al. 1990, Yu et al. 1998) support these findings.

Moisture gradients can also induce permanent slab uplift. The top surface can dry out to a depth of about 2 in., where the moisture content is relatively constant (Janssen 1987, Suprenant 2002) which contributes to slab uplift. It has been reported that an uplift of 0.12 in. at the corners and 0.05 in. at the edge occurred during a period of 40 days (Hatt 1925) for a slab in the laboratory. Poblete et al. (1990) found that slab corners warped upward about 0.05 in. during the dry season in Chile for a 9 in. slab, which is equivalent to the amount caused by a negative temperature gradient of about 0.7°F per inch.

Moisture transport in concrete is limited to a surface region of less than about 3.2 in. in depth (Beddoe and Springenschmid (1999). This is a result of capillary discontinuity, which typically occurs within a week after placement, depending on the water-cementitious ratio, and is a result of the intrinsic hydration property of Portland cement (Powers, 1959). Upward warping can develop if a concrete pavement or floor is subjected to continued exposure to moisture at the bottom (Springenschmid, and Plannerer, 2001, Suprenant 2002).

The magnitude and location of maximum slab stresses change as a consequence of loss of slab support and truck axle loadings. The temperature and moisture conditions resulting in permanently upward-curled/warped slabs are most critical for JPCP. This condition can change the failure mode from bottom-up to top-down transverse cracking, which is typically mid-slab cracking from a combined curl/warp tensile stress, resulting from a loss of support at the joint and mid-slab stresses from multi-axle loading at the unsupported joints.

As an example, I-96, Livingston Co., CS 47065, and I-94, near Watervliet, CS 11017, have developed premature top-down, mid-slab, cracking. The rate of cracking is rapidly accelerating. Their crack development is shown in Figure 1-1.

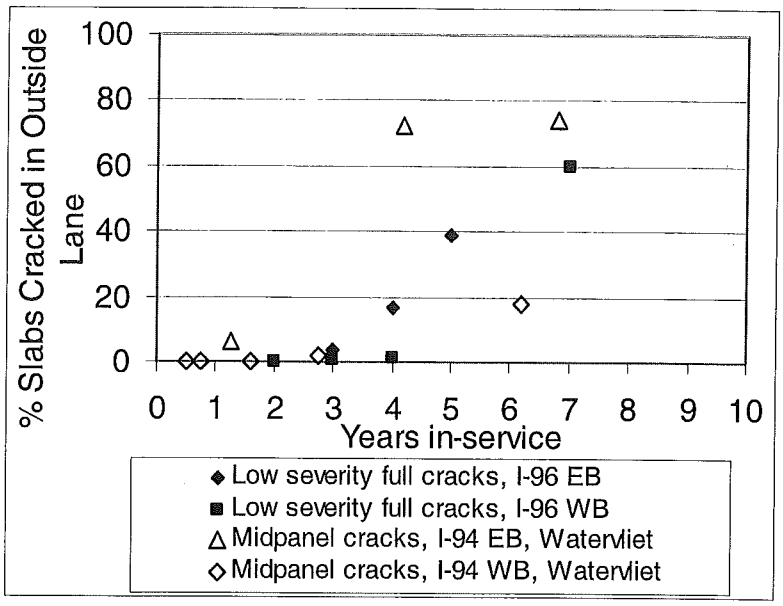

Figure 1-1
Development of top-down transverse mid-slab cracking for two JPCP projects in Michigan (I-96 CS 47065, I-94 CS 11017).

These projects with premature cracking encouraged this research to determine the major factors that contribute to a permanent slab uplift condition, from temperature and moisture gradients.

Project Main Objectives and Benefits of this Study

The study's major objectives are as follows:

1. Determine, from field and laboratory measurements, the magnitude of built-in curl from a temperature gradient and moisture shrinkage gradient for Michigan conditions; and the resulting effect on JPCP resistance to mid-slab, top-down fatigue failure.

2. Establish, based on these results and Finite Element analysis, critical values for built-in curl/warp. These values can lead to development of additional MDOT QC/QA acceptance criteria.

Research Plan

To achieve the major project objectives a number of tasks were undertaken. First, an extensive field and laboratory testing was conducted. For the field testing, two JPCP projects, constructed during summertime and fall time, respectively, were instrumented

with wireless temperature sensors at different depths within a slab's cross section, and the magnitudes of any built-in curl from a temperature gradient at the time of final set were determined. These results are presented in Chapter 2. As part of the laboratory testing a new test procedure for measuring shrinkage-related uplift of a concrete beam, and shrinkage associated with self-desiccation were developed. These results are presented in Chapters 2 through Chapter 3. These results were used as input to a FE program (ISLAB 2000) developed specifically for pavement analysis and presented in Chapter 4. Acceptance criteria for quantifying built-in curl are discussed in Chapter 5 together with project example. Conclusions are presented in Chapter 6. Chapter 7 contains recommendations and implementation of study findings. Testing methods are presented in the appendix.

2.0 LOSS OF SLAB SUPPORT FROM TEMPERATURE CURL

Thermal gradients through the JPCP slab are the most critical climatic inputs for response analysis of PCC pavements. If the top of the PCC slab is warmer than the bottom, a convex curvature results, which, when combined with traffic load, potentially increases bottom-up cracking. If the top of the PCC slab is cooler than the bottom, concave curvature of the slab results, which, when combined with traffic load, potentially increases top-down cracking. From field measurements, built-in curl from time of construction and daily curl are quantified in this chapter.

2.1 Built-in Curl from Time of Construction

Built-in construction curl can be quantified from field temperature measurements of the concrete slab during construction. To demonstrate this, in 2005 wireless temperature sensors were embedded during paving at different depths within a cross section for three pavement reconstruction projects. These projects are the I-94 JPCP Demo Project, CS 82022, located just east and west of Outer Drive Rd, and the US-23 JPCP project, CS 25031, located between Hill Road and Thompson Road. I-96, CS 47065, was instrumented during a preventive maintenance project in 2005. For the I-94 project temperature sensors were installed in the EB direction on June 7, 2005, on a warm, sunny summer day. Temperature sensors for the US-23 JPCP project were installed by the Hill Road exit in the NB direction on October 27, 2005, which was a cool and cloudy day.

The temperature sensors were programmed to collect temperature data from the start of paving in 30-minute intervals. The concrete section used for sensor placement was hand-scooped immediately after placement. The sensors were placed at four different depths at the same location (mid-slab and approximately 2.4 feet from the shoulder) starting from the top of the base, approximately 2 inches, 4 inches, 6 inches, and 8 inches above the slab bottom. The sensor locations are shown in Figure 2-1 for the I-94 demo project. Another sensor was located off the shoulder to record ambient temperature.

The measured temperatures at different depths within the first day after paving are shown in Figure 2-2 for both the I-94 demo and the US-23 JPCP projects. As no temperature sensors were installed at the slab's surface, these temperatures were linearly extrapolated from the two closest sensors below the surface, as shown in dashed lines (Figure 2-2). For summertime construction (I-94), the temperature differences stay positive for most of the first day. For fall construction conditions (US-23), however, the temperature difference shifts from positive to negative shortly after paving.

The temperature difference at the time of final set was found to be of great significance, as it determines the extent of the slab-base contact condition while the pavement is in service. However, the final set time is affected by the concrete's curing temperature: A higher curing temperature leads to earlier final set. A relationship of the final set time and the curing temperature is presented in Figure 2-3, which was determined from mortar specimens according to ASTM C403. This relationship is used to estimate the final set

time of concrete in the field by converting field concrete temperature into a reference temperature (73^0F/23^0C) using the maturity concept (ASTM 1987).

The maturity concept was developed to consider the combined effect of temperature and time on strength gain. The concept is that the same strength is achieved at the same maturity (degree of hydration). Equation (2-1) shows a maturity function based on Arrhenius law:

$$M = \sum_{0}^{t} \exp[-\frac{E_a}{R}(\frac{1}{T} - \frac{1}{T_r})]\Delta t \qquad (2\text{-}1)$$

Where, M = maturity, in hours or days
E_a = activation energy
R = gas constant
T, T_r = temperature at a given time and reference temperature, respectively, in ^oK
Δt = time interval

Based on the field-measured concrete temperature and the maturity concept, the final set time is calculated to be 4.5 hours for I-94 demo project, and 8.5 hours for US-23 JPCP project in this study. Thus, a positive temperature difference of 20°F is measured at the time of final set for the I-94 demo project, as shown in Figure 2-2. This indicates that the slab is flat at final set with a positive temperature difference of 20°F. When the thermal gradient vanishes, the slab will curl up as if it is subjected to a -20°F temperature difference. Thus, the built-in temperature difference (construction curl) is -20°F for this I-94 demo project paved on a summer day in Michigan.

Late fall paving, however, results in a slightly downward permanent curl, as represented by US-23, paved on Oct. 27, 2005. A negative temperature difference of -3°F was found at the time of final set, 8.5 hours after paving. Thus, the slab will curl downward when the thermal gradient is dissipated, and a slight downward curling is permanently "locked into" the slab.

The influence of the built-in curl on the daily temperature difference can be quantified by using an effective temperature difference that is obtained by combining the built-in construction curl with the daily temperature difference in the field slab. The effective temperature difference is written as equation (2-2). The value for $T_{effective}$ can be positive or negative.

$$T_{effective} = (T_{top,daily} - T_{bottom,daily}) - (T_{top,final-set} - T_{bottom,final-set}) \qquad (2\text{-}2)$$

Where

$\Delta T_{effective}$: The effective temperature difference resulting from the combined effects of daily temperature difference and built-in temperature difference.

$T_{top,daily}$: Top surface temperature due to daily environmental temperature cycles.

$T_{bottom,daily}$: Bottom surface temperature due to daily environmental temperature cycles.

$T_{top,final-set}$: Top surface temperature at final set.

$T_{bottom,final-set}$: Bottom surface temperature at final set.

Summer construction subjects concrete pavement to an extended upward curl condition due to a likely negative built-in curl. This is demonstrated in Figure 2-5. The effective temperature difference is plotted along with the daily temperature difference. It is seen that summertime paving can shift the daily temperature gradient below zero, and the effective temperature difference during a 24-hour cycle is negative all the time, indicating a permanent slab uplift condition. According to this figure the most negative temperature difference is approximately -30^{0}F. A -30^{0}F temperature difference within a cross section will result in major slab uplift. This temperature shift is a very significant factor determining whether top-down or bottom-up stress will be more critical. Late fall construction, however, will shift the daily temperature slightly toward the positive direction, which is desirable for the slab's curling conditions.

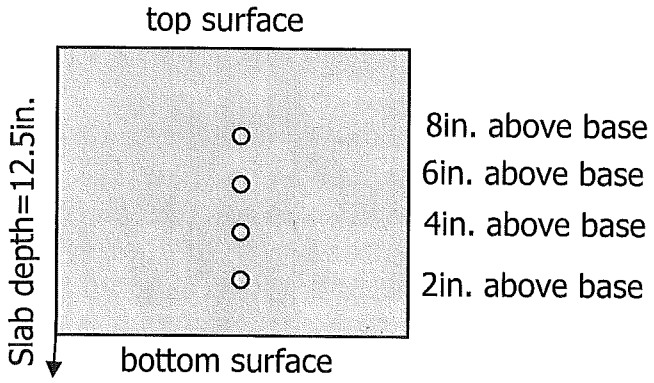

Figure 2-1
Locations of temperature sensors for the I-94 Demo Project, CS 82022,

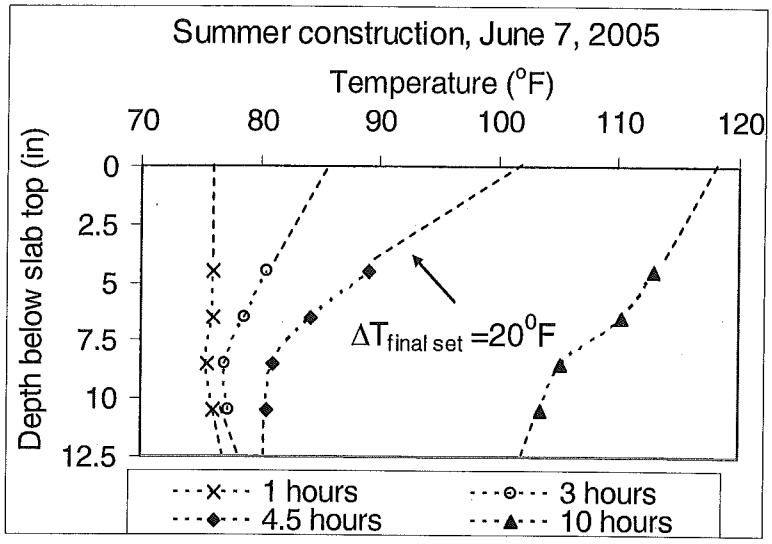

(a) Summer construction

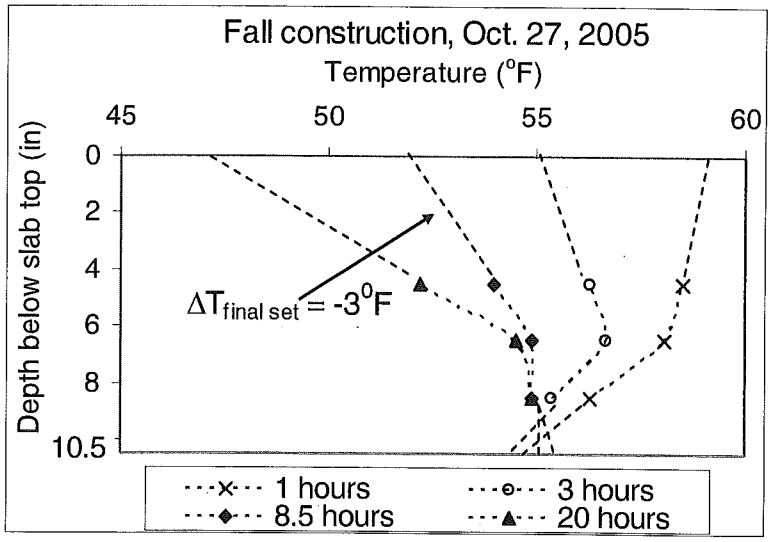

(b) Fall construction

Figure 2-2
Temperature distributions along slab depth after paving (temperature data provided by Tim Stallard, MDOT)

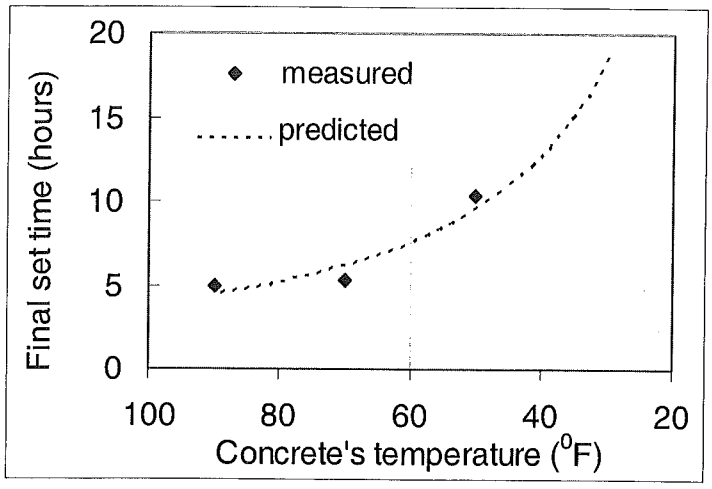

Figure 2-3
Laboratory measured final set time of mortar according to ASTM C403

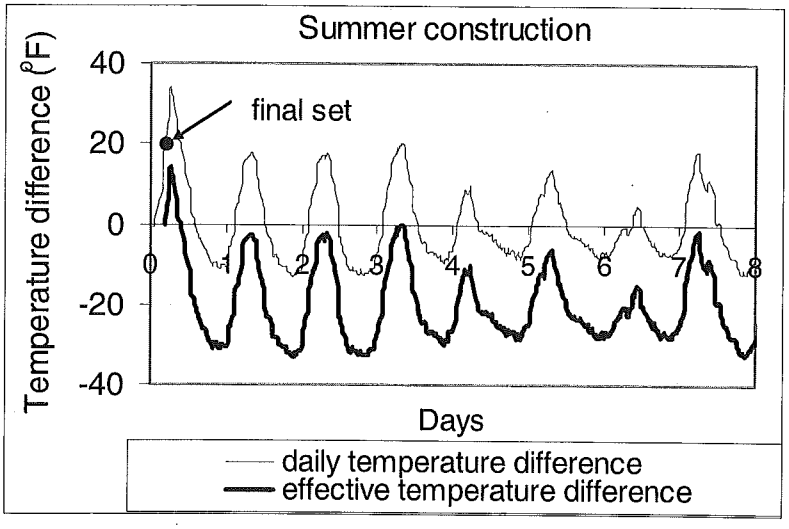

(a) Summer construction

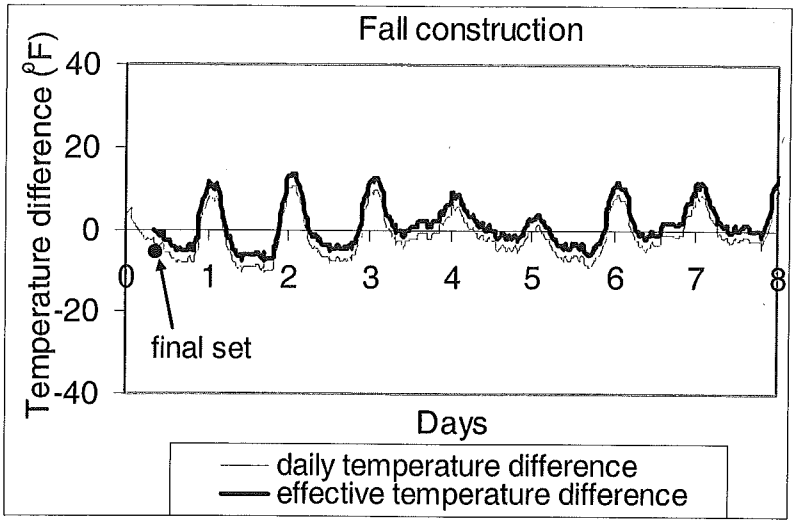

(b) Fall construction

Figure 2-4
Influence of built-in curl on daily temperature difference

2.2 Daily and Seasonal Temperature Curl

Without actual field measurements, normally a maximum temperature gradient of 2.5 to 3.5°F/inch for a slab is assumed during the day and about half that value is assumed at night or for a cloudy/overcast day (Huang 1993).

Temperature gradients vary continually throughout the day and with season.

Long-term pavement temperatures were closely monitored for the field slabs of I-96, CS47065 and US-23, CS 25031, projects by using wireless temperature sensors. The temperature results are presented in Figure 2-5 and 2-6. The top and bottom temperatures were linearly extrapolated from the closest two wireless sensors, as no sensors were installed at the surface.

Based on the field measurements, it was found that the maximum negative temperature difference typically ranges from -12°F to -15°F. The highest measured positive temperature difference was found to be prevalent during spring and summer months. They range from 18°F to 22°F.

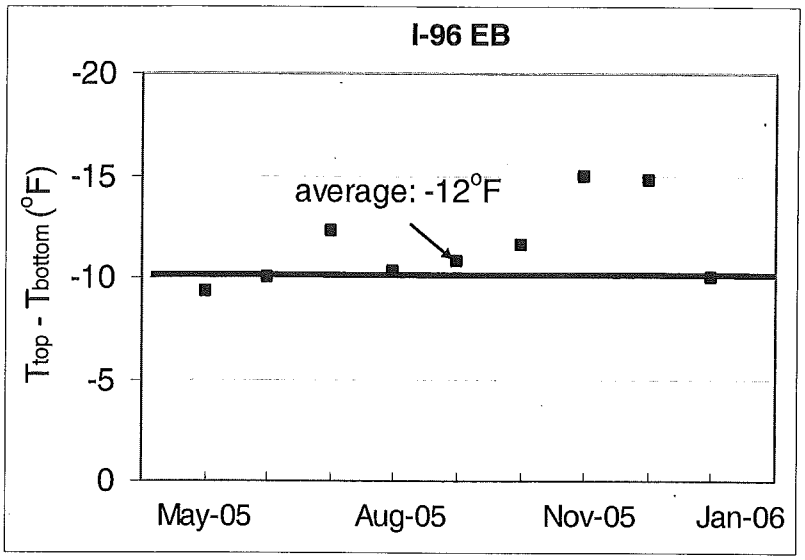

(a) Monthly negative temperature difference

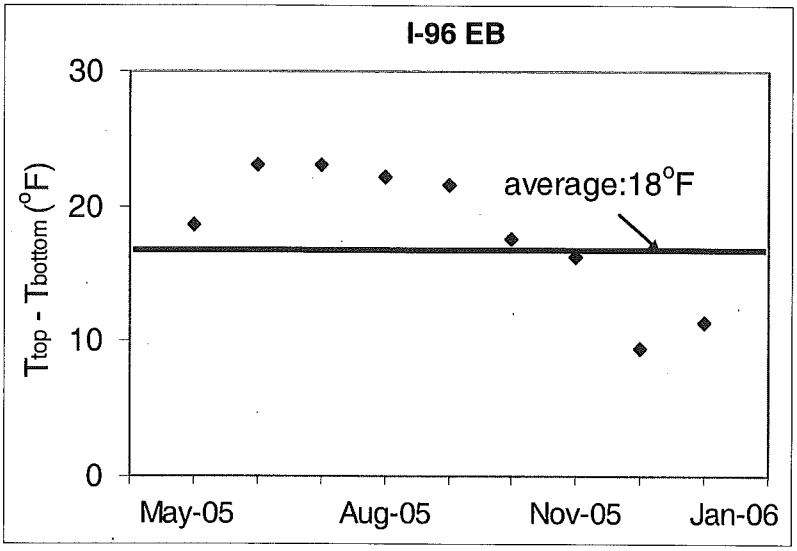

(b) Monthly positive temperature difference

Figure 2-5
Field measured temperatures of I-96 JPCP, CS 47065

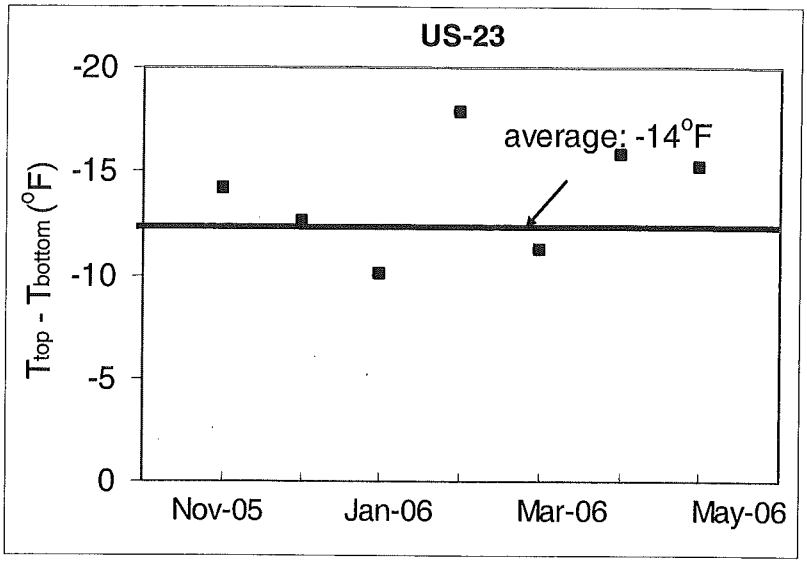

(a) Monthly negative temperature difference

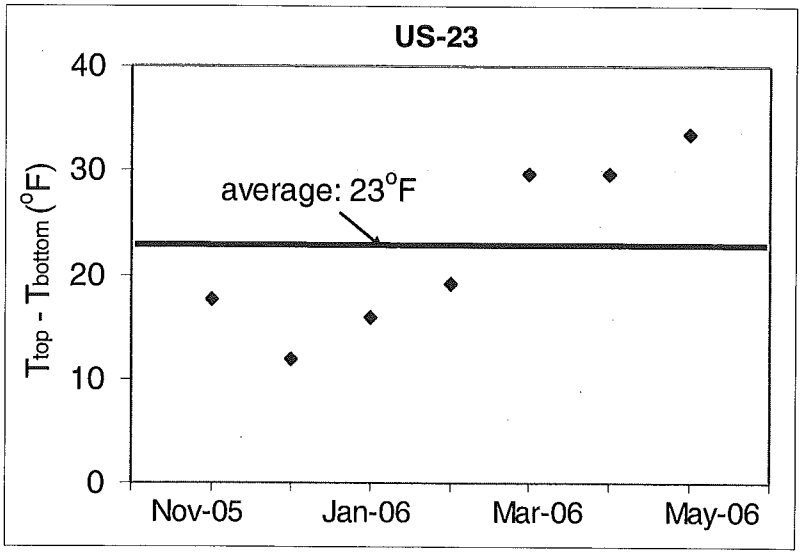

(b) Monthly positive temperature difference

Figure 2-6
Field measured temperatures of US-23 JPCP, CS 25031

3.0 LOSS OF SLAB SUPPORT FROM MOISTURE SHRINKAGE WARPING

As a compounding factor to slab uplift, warping occurs when there is a difference in moisture between the top and bottom surfaces of a concrete slab. Two components contribute to moisture warping. They are (1) drying shrinkage, which is a result of moisture loss from external drying at the slab top. (2) differential autogenous shrinkage from water suction from the base. This chapter presents the laboratory test procedure using beam uplift measurements.

3.1 Drying Shrinkage

The slab top tends to dry out from surface evaporation. About two inches below the surface, however, the moisture level remains at a relatively constant high level. Thus, the top surface shrinks relative to the bottom portion, resulting in an uplift condition as illustrated in Figure 3-1.

It has been reported that an uplift of 0.12 inches at the corners and 0.05 inches at the edge occurred over a period of 40 days' drying for a slab in the laboratory (Poblete et al. 1990). Work by Poblete et al found that slab corners warped upward about 0.05 inches during the dry season in Chile for a 9-inch-thick slab, which is equivalent to the curling caused by a negative temperature gradient of about 0.7°F per inch (Poblete et al. 1990).

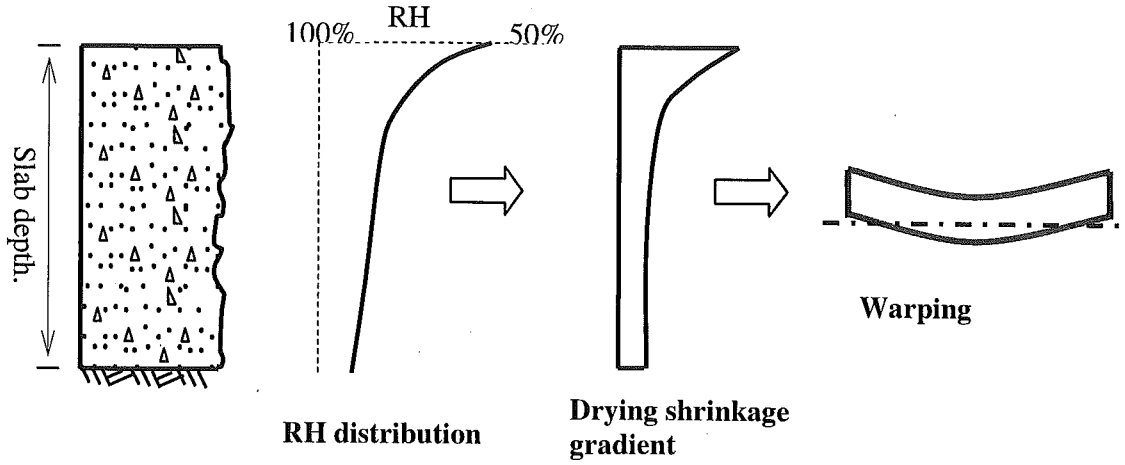

Figure 3-1
Warping of slab from surface drying shrinkage

3.2 Differential Autogenous Shrinkage

Concrete pavements which are subject to drying shrinkage at the top and in contact with moisture at the bottom develop substantial warping (Springenschmid and Plannerer 2001). This added uplift from continued exposure to moisture at the bottom is a result of differential autogenous shrinkage.

Autogenous shrinkage is the macroscopic volume reduction of cementitious systems without moisture transfer to the environment. This property is a result of self-desiccation of pores within the hydrating cement paste, thus increasing with degree of hydration. As long as the concrete surfaces are sealed during hydration, autogenous shrinkage is uniform and thus no warping develops as shown in Figure 3-2. The hydrating cement paste develops capillary discontinuity (Powers et al. 1959). This has been found to hinder moisture transport for travel distance greater than about 3 in. (80 mm) (Beddoe and Springenschmid 1999). Once this happens, a moisture gradient can develop within the cross section any time the concrete is exposed to water at a free surface, which causes a differential autogenous shrinkage strain and warping. Figure 3-2 illustrates this phenomenon.

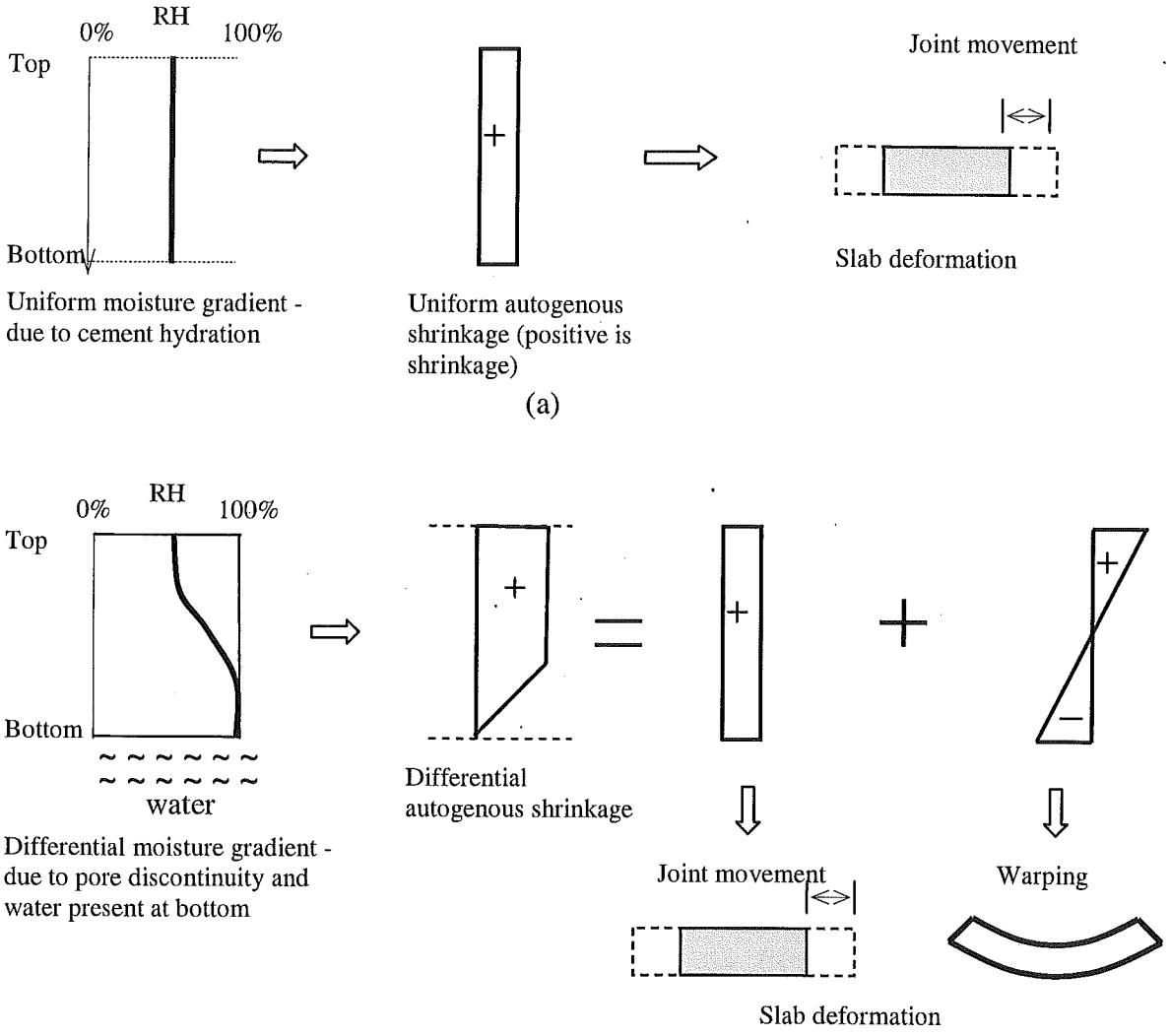

Figure 3-2
Sketch illustrating uniform shrinkage for sealed curing and differential Autogenous shrinkage from wetting at the bottom

3.3 Laboratory Testing and Results

To simulate uplift from a moisture gradient between slab top and bottom, moisture warping of a concrete beam was measured for MDOT standard P1 mixture containing coarse aggregate (Bruce Mines with water absorption of 0.3%).

3.3.1 Test setup

A test setup was developed at U of M based on Springenschmid's work as shown in Figure 3-3 (Springenschmid, and Plannerer 2001). This test can simulate beam uplift

from simultaneous drying from top surface evaporation and water suction at the bottom. The concrete beam was 7.5 ft. in length, 8 in. in depth, and 6 in. in width. One end of the beam was fixed, and the other end was free to lift up. A dial-gauge was installed at the free end to record the amount of moisture warping over time. To facilitate a moisture gradient through the thickness, the two sides of the beam were sealed using water-proof paint. The whole test setup was stored in an environmental chamber with constant relative humidity (50%) and air temperature (73^0F). The measurement was initiated at the age of 7 days, when concrete has gained enough strength to lift up. Before initiating the test, the concrete beam was sealed and cured for 7 days in the environmental chamber.

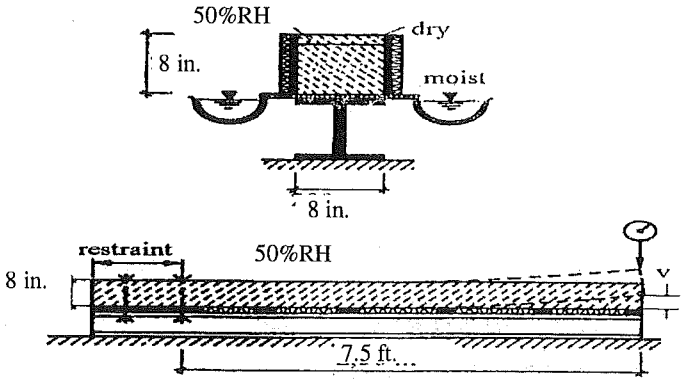

(a) Beam warping test by Springenschmid Plannerer

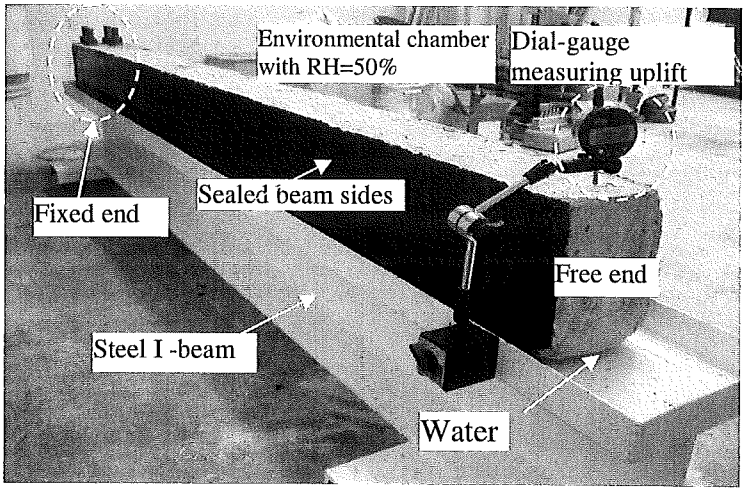

(b) U of M test set up

Figure 3-3
Laboratory moisture warping test

3.3.2 Results

Moisture warping tests were conducted on concrete beams for two probable moisture conditions existing with a field slab (Figure 3-4): (a) drying at top and water present at bottom, corresponding to the case of a field slab resting on a saturated base and drying occurring at the top; (b) drying at the top with the bottom sealed to ensure only moisture loss from the top surface. Two beams were measured for each moisture condition and the amounts of uplift over time are plotted in Figure 3-5.

It was found that warping of the concrete beam is the greatest when there is drying at the top and water present at the bottom. The measured moisture warping increases over time and reaches a plateau after 55 days of testing. The total moisture warping for the two sources combined is 90 mils (2.3 mm), average of two tests, whereas drying shrinkage contributed only 16 mils (0.4 mm).

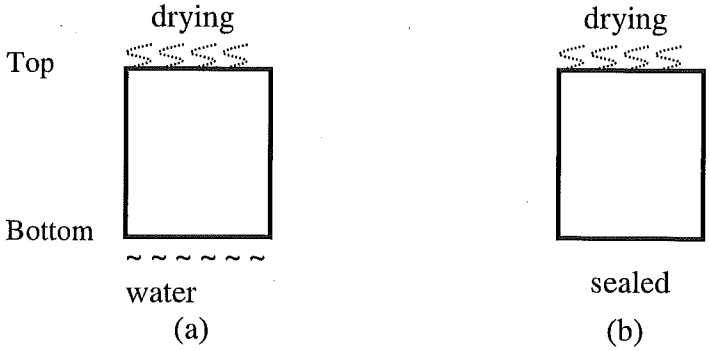

Figure 3-4
Two moisture conditions simulated in beam warping tests

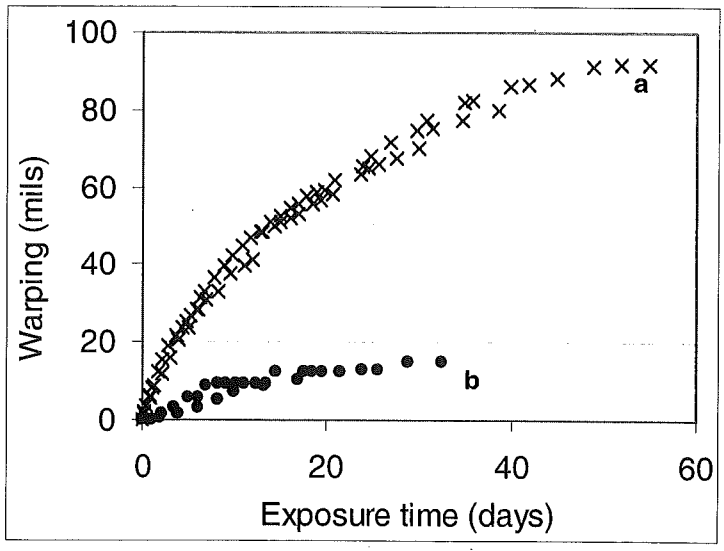

Figure 3-5
Beam warping results for two conditions, (a) combined drying and wetting, and (b) drying only.

3.4 Equivalent Linear Temperature Difference from Differential Autogenous Shrinkage

Differential autogenous shrinkage is a cement-hydration-related material property. In order to evaluate its effect on pavement performance it is useful to quantify differential autogenous shrinkage by using an equivalent linear temperature difference (ELTD). This equivalent linear temperature difference is the input for a commercial Finite Element Analysis (FEA) software ISLAB2000 used in this study to predict slab uplift and fatigue stress. The ELTD for differential autogenous shrinkage can be added to the other three factors (i.e. daily temperature difference, built-in temperature difference from construction curl, and moisture related ELTD from drying shrinkage). Figure 3-6 illustrates the procedure of converting the effect of differential autogenous shrinkage to an ELTD (ΔT). The basic principle is to assume that the moment (M_2) which causes uplift due to an ELTD is equal to the moment (M_1) induced by differential autogenous shrinkage strain. The moments M_1 and M_2 here are calculated from the strain distribution instead of stress distribution. They are relative to the mid-depth line as marked in Figure 3-6. Therefore, the concrete modulus is not involved. According to Beddoe and Springenschmid (1999), moisture transport is hindered at depths greater than about 3 in. (80 mm) due to pore discontinuities. Thus, for a slab with its bottom in contact with water, the differential autogenous shrinkage is uniform for the top portion, which equals to the autogenous shrinkage δ. And then it falls to zero starting about 3 inches above the bottom due to the availability of water which fills the capillary pores and thus eliminate autogenous shrinkage strain as shown in Figure 3-6.

The parameters needed to calculate ELTD due to differential autogenous shrinkage are the autogenous shrinkage of concrete, the slab thickness, and the Coefficient of Thermal Expansion (CTE) of concrete. Autogenous shrinkage (the detailed test method can be found in Appendix) was measured for concrete with w/c=0.35 and 0.45, as plotted in Figure 3-7 on a logarithmic time scale. Long-term autogenous shrinkage of w/c=0.45 concrete is extrapolated from short-term measurements, which is used to calculate ELTD. CTE of concrete is assumed as $5 \times 10^{-6}/^{0}F$

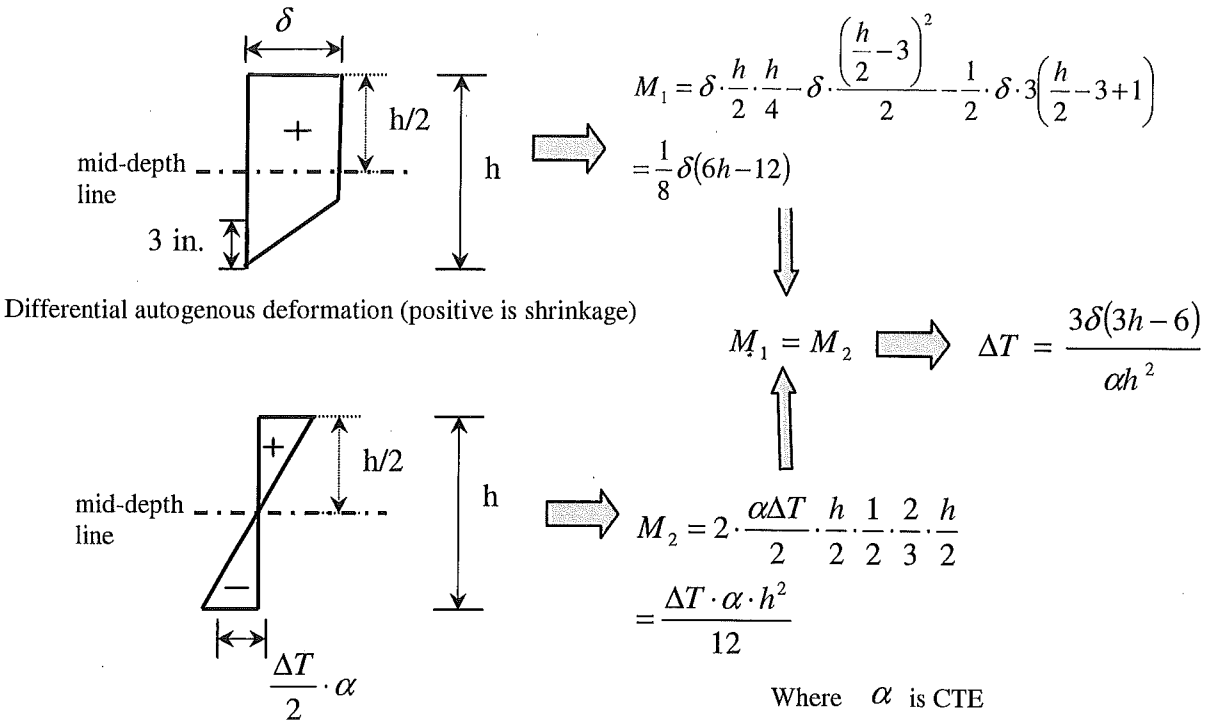

Figure 3-6
Conversion of differential autogenous shrinkage to an equivalent linear temperature difference

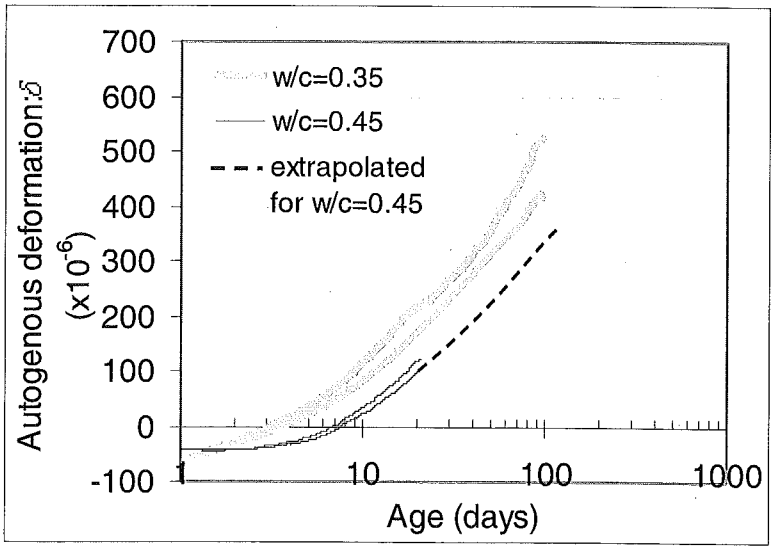

Figure 3-7
Measured autogenous shrinkage of concrete

Figure 3-8 illustrates the predicted ELTD from differential autogenous shrinkage over time. The results show that ELTD is approximately-30^{0}F within a month. After six months of continued exposure to wetting the ELTD ranges from -50^{0}F to -70^{0}F depending on slab thickness. This compounds the temperature curl (built-in curl and daily curl) leading to a larger slab uplift. Not only can this condition increase mid-slab stresses but it may cause pumping of fines into the base and/or base erosion.

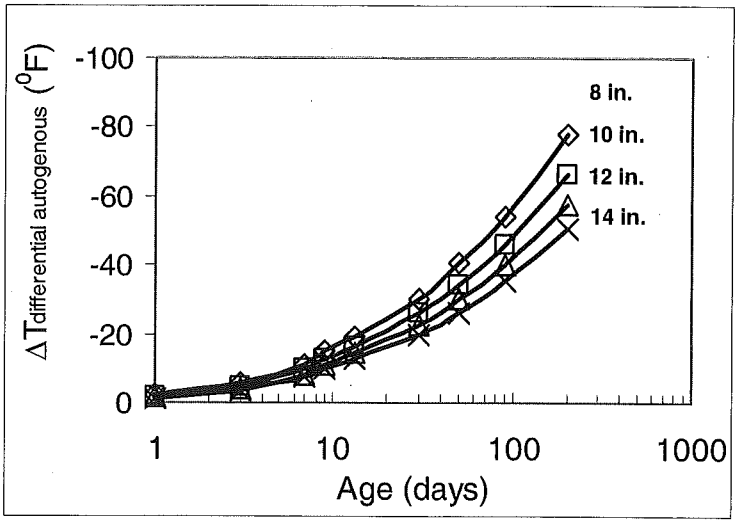

Figure 3-8
Equivalent linear temperature differences from differential autogenous shrinkage for different slab thickness

4.0 FINITE ELEMENT ANALYSIS OF SLAB STRESS FROM CURLING/WARPING GRADIENTS AND TRUCK LOADING

The combined effects from truck loading and loss of slab support at joints from combined temperature curling (built-in and daily) and moisture warping can result in detrimental tensile stresses leading to top down midslab transverse cracking for a 15 ft JPCP on unbound OGDC base.

4.1 Critical TELTD values for 15 ft. JPCP on Unbound OGDC Base

Slab uplift from curl and warp can be quantified by means of single factor referred to as the total equivalent linear temperature difference (TELTD). This term is the cumulative value at a given time. It consists of two thermal components and two moisture shrinkage components as defined in equation 4-1

$$TELTD = \Delta T_{daily} + \Delta T_{\substack{built-in \\ temperature}} + \Delta T_{drying} + \Delta T_{differential-autogenous} \qquad (4\text{-}1)$$

Where, ΔT_{daily} is the daily positive or negative temperature difference and $\Delta T_{\substack{built-in \\ temperature}}$ is the positive or negative built-in curl from a temperature gradient at final set. Since moisture gradients are not known, the uplift from moisture effects is conventionally converted to an equivalent temperature gradient. Thus, ΔT_{drying} is the equivalent negative temperature difference from drying shrinkage and $\Delta T_{differential-autogenous}$ is the equivalent negative temperature difference from differential autogenous shrinkage.

4.1.1 Daily Curl

The daily curl component is not possible to control as it occurs naturally from changing environmental factors. Still, it is an important factor that needs to be included in the TELTD value. For Michigan environmental conditions daily curl is shown between 6 am and 12 noon. During this time period it ranges from -10^0F to 15^0F based on field measurements of instrumented slabs of the I-96 JPCP project (CS 47065), per Figure 4-1.

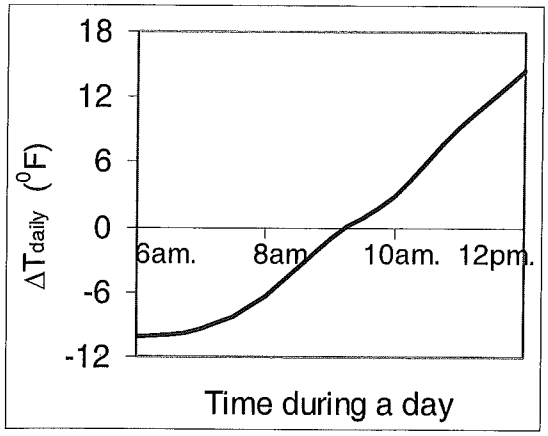

Figure 4-1
Daily temperature difference between 6am.and 12noon of I-96 JPCP project, CS 47065

4.1.2 Built-in Construction Curl

The built-in temperature curl is a function of temperature gradient at final set, and thus depends on several factors such as base and air temperature, time of day of placement, concrete initial temperature and slab thickness. In summary, it was found to vary from a high of 20^0F (equivalent -20^0F) during summertime construction to -3^0F (equivalent $+3^0$F) for late fall as shown in Figure 4-2 (a) and b).

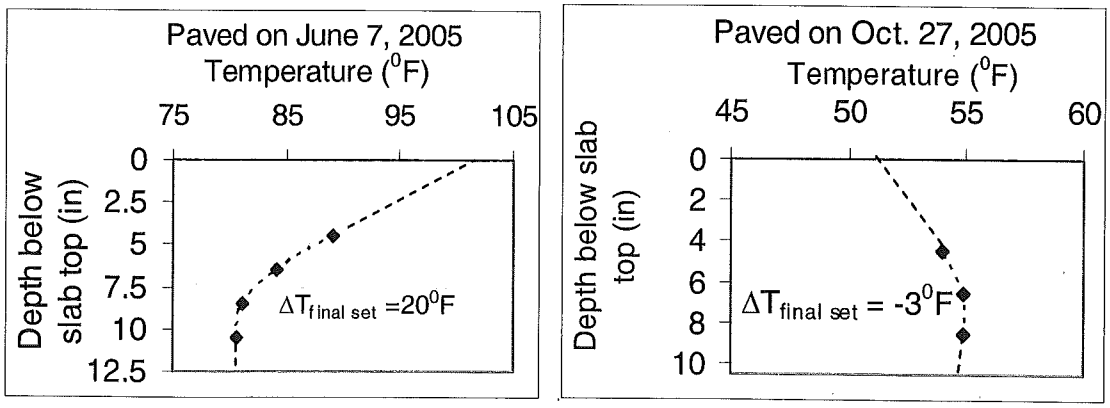

(a) Summertime construction; (b) fall construction

Figure 4-2
Built-in temperature gradient at time of final set

4.1.3 Equivalent Linear Temperature Difference from Differential Autogenous Shrinkage

The equivalent temperature difference from differential autogenous shrinkage, $\Delta T_{differential-autogenous}$, was estimated using the procedure described in section 3.4.

The magnitude was found to depend on the exposure time to water at the beam bottom and water-cement ratio. The laboratory measured autogenous shrinkage from this study is illustrated in Figure 3-7 (Chapter 3). The equivalent linear temperature difference (ELTD) from differential autogenous shrinkage is estimated versus time from beam uplift results and plotted in Figure 3-8. It is seen that $\Delta T_{differential-autogenous}$ increases over time because autogenous shrinkage increases over time.

Strictly speaking, $\Delta T_{differential-autogenous}$ predicted in Figure 3-8 is for beam uplift. However, it can still be approximated as mid-slab joint uplift because modulus of subgrade reaction, k, does not have a big influence on uplift once it exceeds 250 pci (Hansen et al. 2007).

4.1.4 Equivalent Linear Temperature Difference from Drying Shrinkage

Beam test results suggest that moisture warping uplift from drying shrinkage alone is small in comparison to uplift from differential autogenous shrinkage.

4.2 Critical Total Equivalent Linear Temperature Difference (TELTD)

Onset of fatigue cracking starts at about a 45% flexural stress-to-strength ratio. These values are shown in Table 4-1. Increasing slab thickness can resist larger TELTD values while higher CTE reduces TELTD. Elastic modulus is another key factor. For example, a 10-in.-thick slab is expected to withstand a TELTD value ranging between -25 to -65^{0}F depending on CTE and modulus value (E as measured and Effective E) used in the analysis. It is emphasized that creep and associated stress relaxation effects are typically unknowns and in the analysis creep effects are approximated using a reduced E-value. In this study an effective E-value of 50% of measured E was assumed.

The results in Table 4-1 suggest that TELTD from thermal effects are not sufficient for top-down mid-slab cracking for Michigan environmental conditions as long as slab thickness is 10 inches or greater. Moisture warping effect on TELTD from prolonged exposure to water at the slab bottom is required. These predictions further suggest that concrete CTE is a factor as well.

Table 4-1
Predicted TELTD to stay below the fatigue limit

Slab thickness (in.)	TELTD (^{0}F) (effective modulus: 2x10^6 psi)		TELTD (^{0}F) (Young's modulus: 4x10^6 psi)	
	CTE=4x10^{-6}/^{0}F	CTE=6x10^{-6}/^{0}F	CTE=4x10^{-6}/^{0}F	CTE=6x10^{-6}/^{0}F
8	-50	-30	-25	-15
10	-65	-40	-35	-25
12	-100	-65	-65	-45
14	-150	-110	-130	-80

4.3 Finite Element Analysis of Total Slab Stresses.

The Finite Element (FE) program ISLAB2000 was used to determine pavement's response to environmental conditions and traffic loadings. Plate theory (Huang 1993) is utilized in ISLAB2000 to determine stresses and deflections. ISLAB2000 enables modeling of multiple slabs with aggregate interlock and/or dowels between slabs for load transfer. Multiple loaded areas can also be analyzed. The required inputs include pavement layer properties, slab dimension, load transfer efficiency, axle loading-location, and concrete properties, such as Coefficient of Thermal Expansion and Young's modulus.

4.3.1 Influence of truck configuration on total stress

The magnitude of fatigue stress varies substantially depending on the type of trucks. Three types of trucks (typical 11-axle truck, 6-axle truck and 5-axle (FHWA) truck, as shown in Figure 4-3) were selected for fatigue stress modeling. The critical loading positions of these three trucks were determined for JPCP by moving the axles in the traffic direction in 20-inch increments to find the location corresponding to the maximum tensile stress.

To assess the total stress under these three trucks, the input parameters to ISLAB2000 were as follows: slab length was 15 ft; slab thickness was 10in.; Young's modulus, E, was 3.6×10^6 psi; the Coefficient of Thermal Expansion (CTE) of the concrete was 5.5×10^{-6} /°F; the subgrade reaction k was 250 pci; the negative temperature difference was -20^0F; and the joint load transfer efficiency was 100% for all slabs. Load-transfer between the slab and shoulder was ignored in the analysis.

The stress contours at the top of the slab for each of the truck loadings are shown in Figure 4-3. Maximum tensile stresses range between 230 to 240 psi. The critical fatigue stresses are located at mid-slab edges, extending toward the slab center with decreasing magnitude, in agreement with established theory.

The 5-axle truck causes slightly higher total stress than the other two trucks. On the other hand, the cumulative fatigue damage in terms of top-down cracking caused by the 11-axle and 6-axle truck loadings may be larger than the 5-alxe truck as the slabs are subjected to the maximum mid-slab stress three times for each pass of the 11-axle or 6-axle truck.

In the following sections, the 5-axle truck loading is used for total stress predictions.

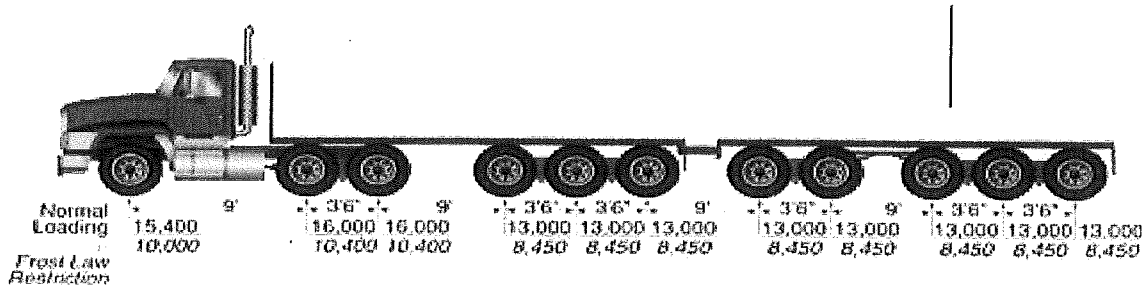

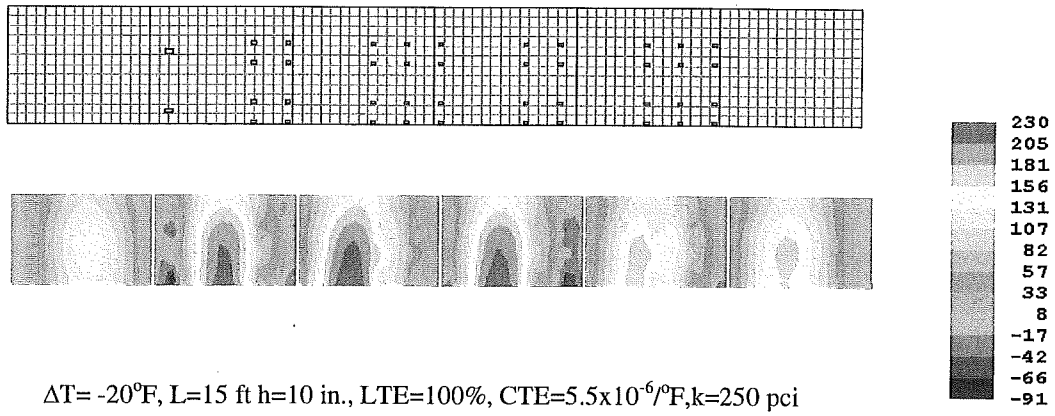

ΔT= -20°F, L=15 ft h=10 in., LTE=100%, CTE=5.5x10^{-6}/°F,k=250 pci

(i) Typical 11-axle (gravel haul) truck loading

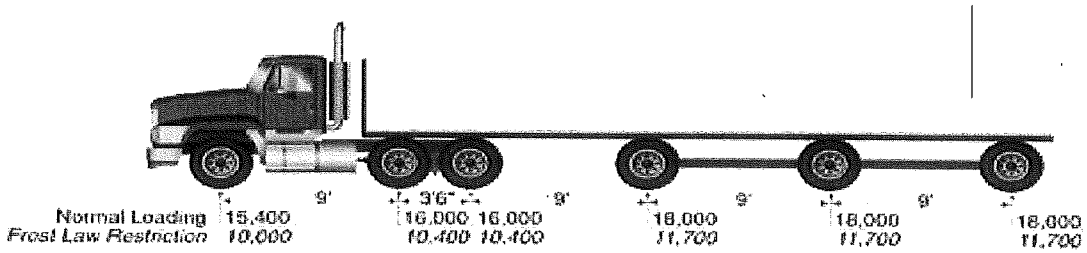

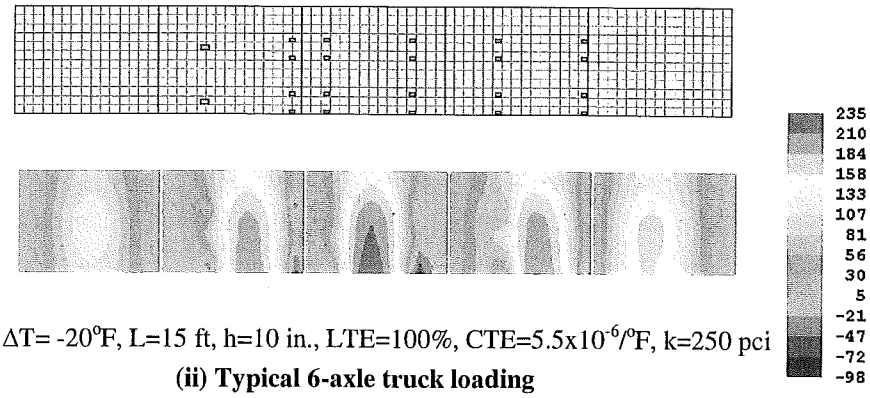

ΔT= -20°F, L=15 ft, h=10 in., LTE=100%, CTE=5.5x10^{-6}/°F, k=250 pci

(ii) Typical 6-axle truck loading

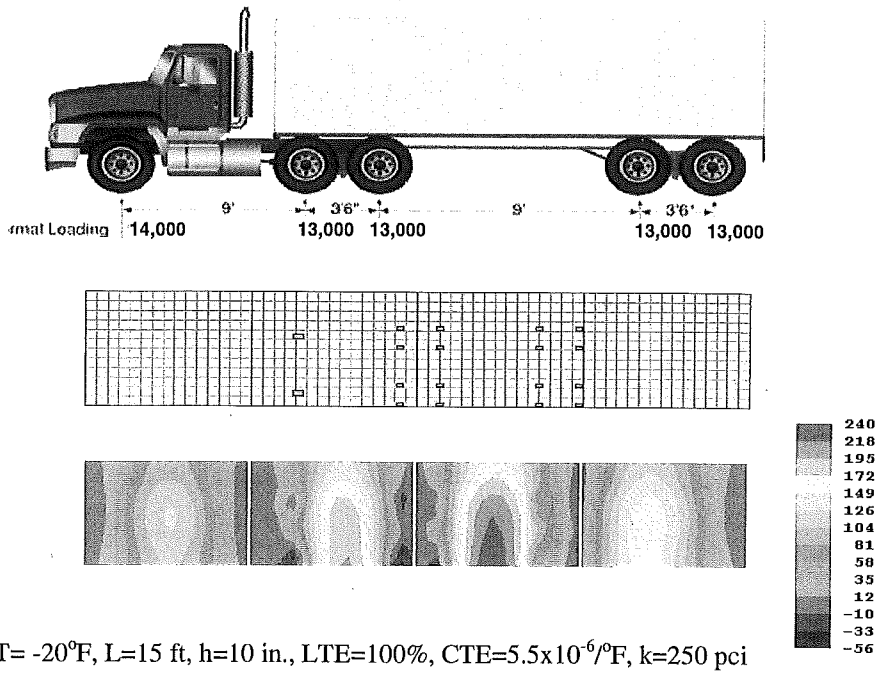

ΔT= -20°F, L=15 ft, h=10 in., LTE=100%, CTE=5.5x10^{-6}/°F, k=250 pci

(iii) 5-axle truck loading

Figure 4-3
Stress contours at slab surface under negative temperature gradient and truck loadings for JPCP

4.4 Predicted Flexural Stress Ratio from Negative Temperature Gradient and Truck Loadings

It is generally agreed that mid-slab cracking of concrete pavements is fatigue related. For fatigue cracks to initiate a stress to strength ratio of 0.45 or greater is typically assumed.

An important concrete property for stress analysis is creep and corresponding stress relaxation. A creep and relaxation-adjusted modulus can range from 20 to 70% of the elastic modulus (Suprenant 2002). This study assumes an effective modulus that is 50% of the static modulus.

The flexural stress ratio curves were predicted and compared with a 650 psi flexure strength in order to assess the cracking risk. The input parameters for the prediction using ISLAB are: TELTD values for concretes with low (4 x 10^{-6}/^{0}F) and high CTE (6 x 10^{-6}/^{0}F), low concrete modulus (2 x 10^6 psi) for creep effect and regular modulus (4 x 10^6 psi) for analysis without creep. Slab thickness ranged from 8 in. to 14 in. The subgrade reaction *k* was 250 pci typical for unbound OGDC. Load transfer efficiency of 100% was used in the analysis.

The predicted stress ratios versus TELTD are shown in Figure 4-4 (a-d) for the two combinations of CTE and E-value which should cover the spectrum of concrete

properties. The dashed lines are the flexural stress ratios representing fatigue-crack initiation risk.

If relaxation is considered in the stress analysis, fatigue crack initiation is predicted for TELTD values exceeding -60^{0}F for a 10-in.-thick slab, increasing to -100^{0}F for a 12-in.-thick slab. Thus, built-in construction curl (-20^{0}F) and daily curl (-10^{0}F) combined are not sufficient to cause top-down cracking in slabs thicker than 10 inches. Therefore, TELTD from moisture shrinkage warping is a requirement for top-down cracking.

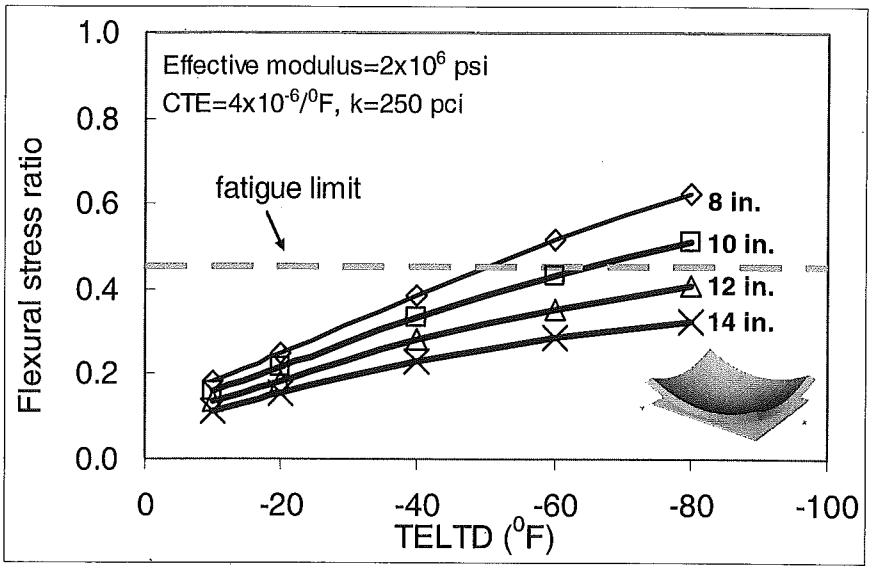

(a) low CTE, effective modulus with consideration of relaxation effect

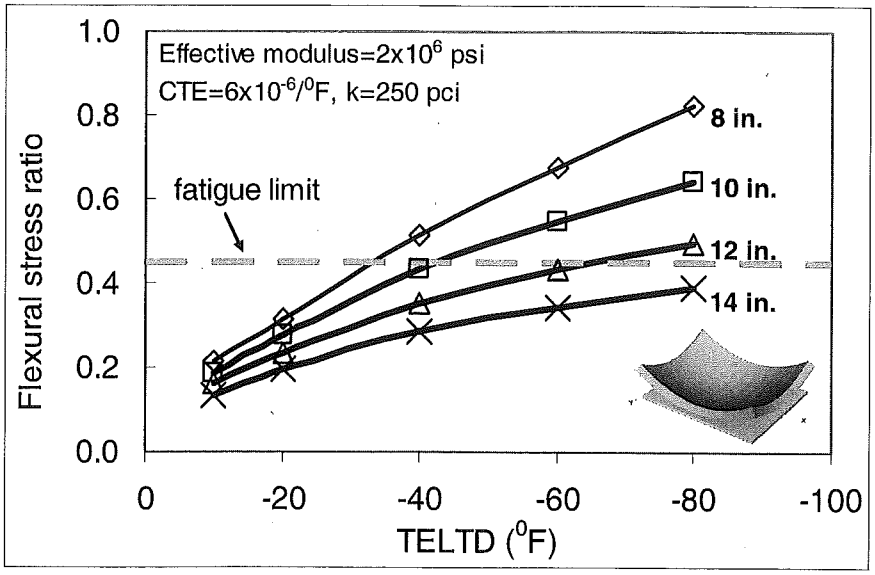

(b) High CTE, effective modulus with consideration of relaxation effect

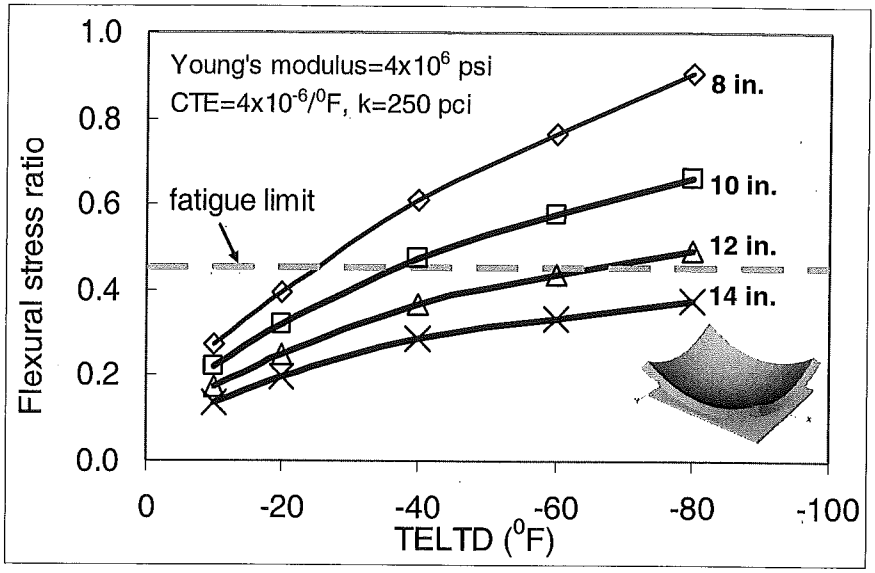

(c) Low CTE, Young's modulus without consideration of relaxation effect

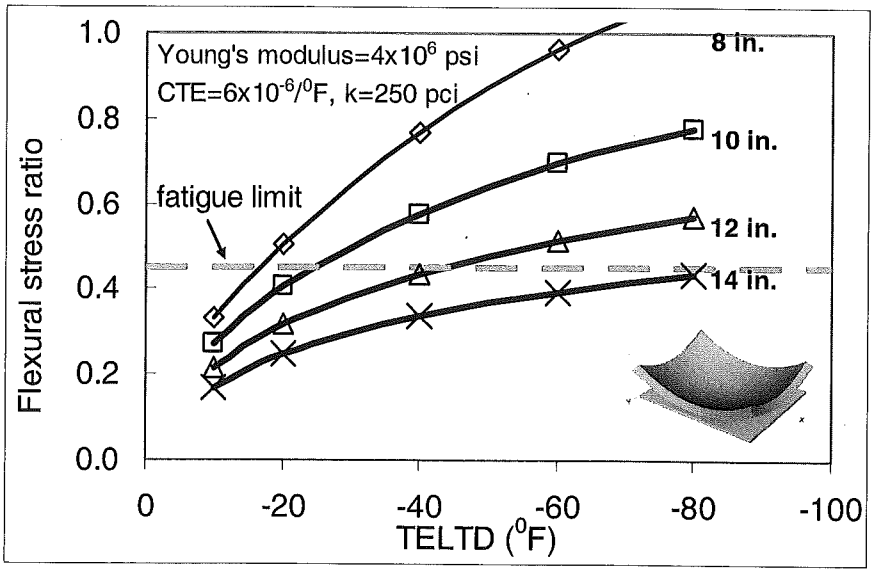

(d) High CTE, Young's modulus without consideration of relaxation effect

Figure 4-4
Flexural stress ratio associated with top-down cracking in JPCP due to TELTD with a 5-axle truck loading

5.0 ACCEPTANCE CRITERIA FOR QUANTIFYING BUILT-IN CURLING

Slab profile measurements are used as input to ISLAB 2000 for estimating TELTD values, as explained in Chapter 4. In the following section a practical methodology is presented based on Finite Element analysis for assessing the slab uplift condition at a given time. Slab uplift is affected by ELTD contributors (two thermal and two shrinkage as discussed in Chapter 4). Knowing slab uplift is the basis for a specification for pavement acceptance when built-in curl has been confirmed. The following section presents limits for uplift (difference in surface elevation between outer corner and mid-edge).

5.1 Risk Assessment

Slab uplift is a useful and practical parameter to assess fatigue risks as it can be monitored and measured over time. As previously discussed, two thermal and two moisture factors can contribute to slab uplift. Daily temperature curl changes hourly to adapt to the environment, while the other three factors have long-term effect on slab uplift. As a fixed value from construction, built-in temperature curl starts to level off and may even reduce after the first few days after construction when concrete's stiffness has been fully developed and creep is involved due to slab's self-weight and restraint to uplift at joints. Drying shrinkage will increase amount of uplift from the temperature built-in curl according to the experimental results obtained in this study from laboratory beam tests. Further, beam uplift results show that continued exposure to water at the bottom is a major factor and can be larger than the other three components together. This is illustrated schematically in Figure 5-1.

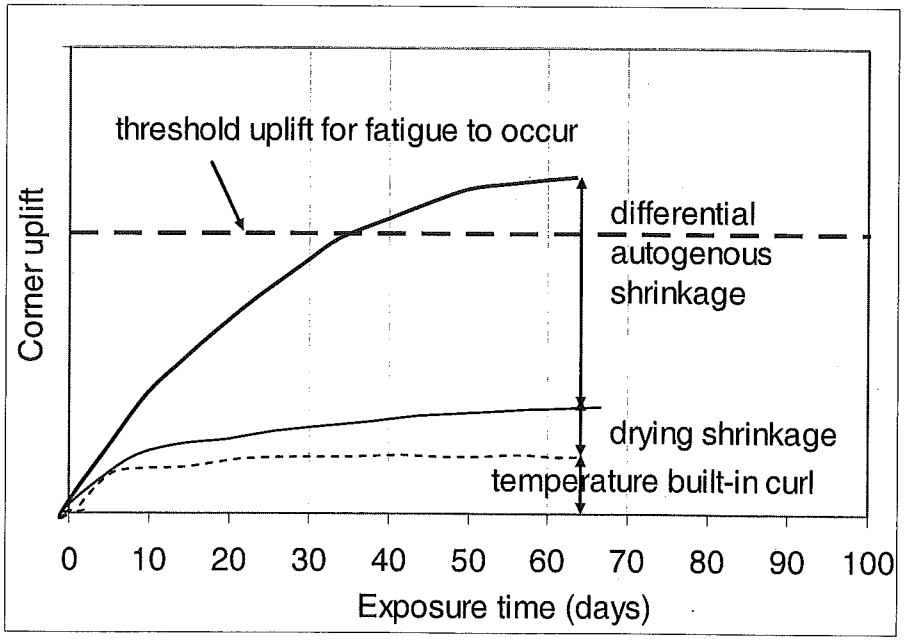

Figure 5-1
Schematic illustration of corner uplift from different types of contributors

Figure 5-2 illustrates the uplift limits versus slab thickness predicted by ISLAB 2000, and considering creep effects (i.e. a 50% reduction in E-value). For example, for a 10-in.-thick slab fatigue cracking can develop if the corner uplift exceeds 0.07 in increasing to 0.120 in. if creep is considered. In view of the complexity in predicting creep effects the critical uplift value, corresponding to the lower fatigue limit, is somewhere in between these two limits. If the uplift of a 15 ft JPCP on granular base exceeds this range at any given time, fatigue is expected to kick in initially causing partial depth cracking at outer edge and midslab, where combined slab stresses are maximum.

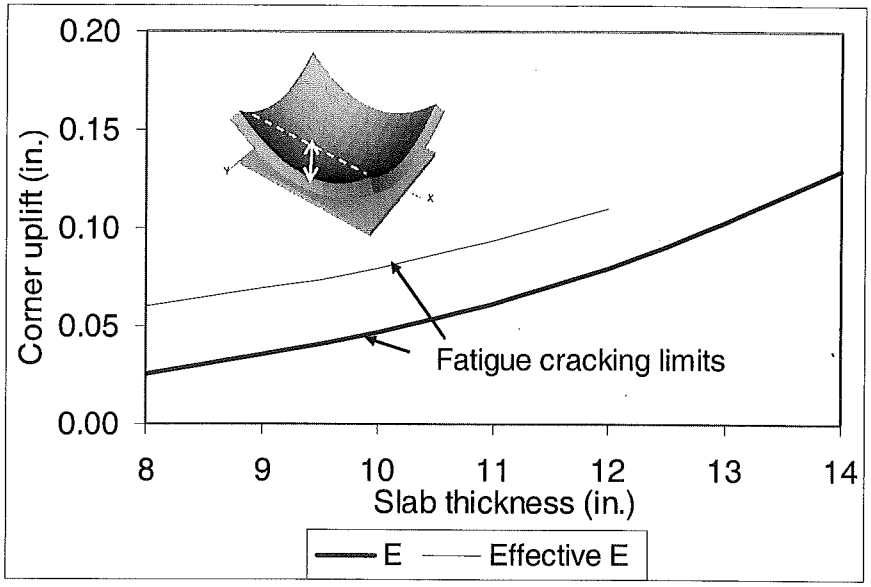

Figure 5-2
Corner uplift limit to initiate fatigue cracking

5.2 Project Example/Case Study I-96, Livingston Co.

A JPCP project constructed in 1996-1998 is located on I-96, CS 47065, Livingston Co. Each direction has three 12 ft lanes with a 10 ft PCC shoulder. Joint spacing is 15 ft. The slab thickness is 10.5 inches. The concrete is a 35 P with blast-furnace slag coarse aggregate. The base consists of a 4 inches 3G OGDC placed on a 3 inch dense-graded aggregate separator course over a nominal 10 inch sand subbase. The subgrade soil consists of a well mixed glacial till of sand to clay.

Surface elevation measurements along the outer edge, lane marking of west bound were taken on warm sunny days during June and July 2005. Slabs were found to be in a permanent upward-concave condition for a series of visibly uncracked slabs, as seen from Figure 5-3. The uplift ranged from 0.08 – 0.20 in. Slab rocking and joint slamming was pronounced when truck axles crossed the joints.

Example of best fit curves through FE analysis is shown for both measured and effective modulus. The back-calculated TELTD values range between -60^{0}F and -85^{0}F for

effective modulus of 2×10^6 psi; and -50^{0}F and -75^{0}F for Young's modulus of 4×10^6 psi for a core-measured CTE value of $5.5\text{x}10^{-6}/^0$F.

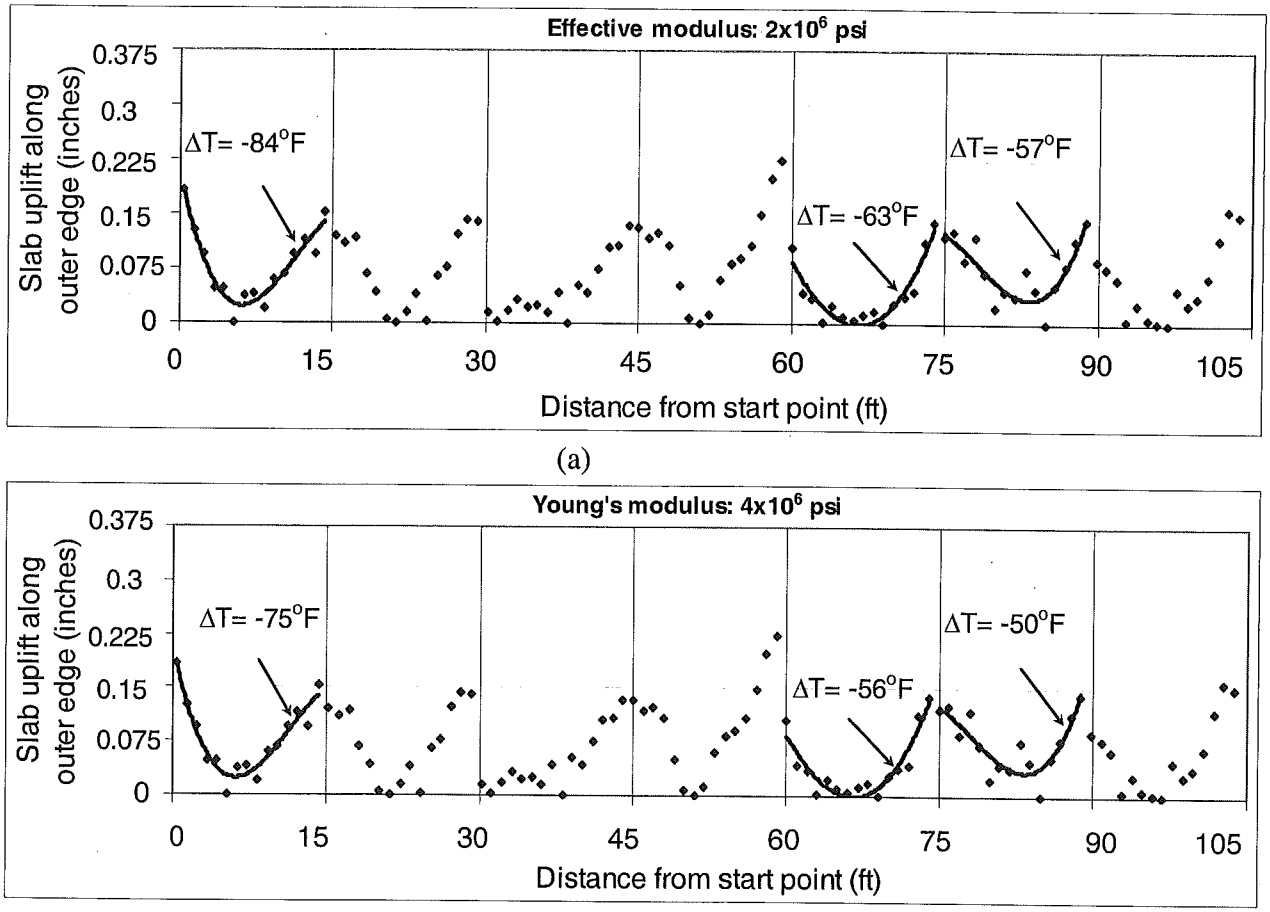

Figure 5-3 Surface elevation profiles for WB I-96 JPCP, CS 47065 with corresponding calculated TELTD values

Base on the predicted TELTD in Figure 5-3, the risk of top-down fatigue cracking for westbound I-96 was assessed in terms of flexural stress ratio (see Figure 5-4). These predicted limits suggest that crack initiation leading to reduced fatigue life occurs at a TELTD of -30^{0}F (without creep effect) and -50^{0}F (with creep effect).

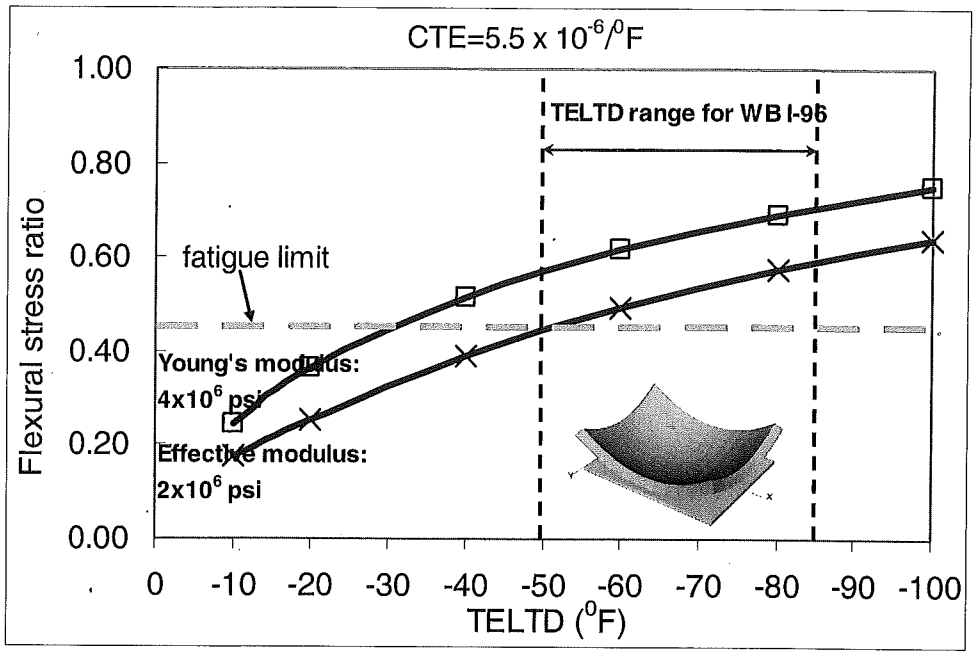

Figure 5-4
Predicted risk of cracking for WB I-96 JPCP project

6.0 CONCLUSIONS

In this study, the cause and effect relationship between built-in upward curl and risk of top-down mid-slab cracking was investigated for JPCP. The investigation included field and laboratory measurements. Based on Finite Element analysis the total equivalent linear temperature difference (TELTD) between slab top and bottom was used as a cumulative measure of slab uplift. It has four components. They are: built-in curl from construction, daily curl, built-in moisture warping from drying shrinkage and differential autogenous shrinkage. Each component temperature difference values are estimated with and without creep effect. Creep causes stress relaxation. The effect of creep on TELTD was accounted for by reducing the elastic modulus value of concrete. The major findings are:

- The combined effects of the four components (thermal and moisture shrinkage) which will reduce fatigue life can be determined from Finite Element analysis by means of a single parameter. This parameter, referred to as negative total equivalent linear temperature difference (TELTD) between a slab top and bottom, is used to assess the combined contribution from each factor (built-in curl from construction, daily curl, built-in moisture warping from drying shrinkage and differential autogenous shrinkage, and creep):

  Built-in Construction Curl: Two projects were instrumented with wireless temperature sensors located at different depths within a cross section. The results show that summertime paving in Michigan can result in a built-in equivalent temperature difference of -20^0F at time of final set known as construction curl. Thus, maintaining a uniform temperature within a concrete cross section until time of set is a factor to consider during summer-time paving conditions. Fall paving conditions in Michigan were found to be favorable to this effect as a cooler surface temperature condition at time of final set will promote a downward concave slab condition. Results show that the built-in curl for the late Fall project ranged from $+ 3^0$F to 0^0F.

  Daily Curl: Temperature results collected over nearly one year from the wireless sensors show that the average daily negative curl (i.e. bottom surface warmer than top) is about -13^0F during the summer and fall months.

  Built-in Moisture Shrinkage Warping: This factor can have two contributors, which both increase over time. Moisture warping from exposure to water at the slab bottom can be the major cause of mid-slab cracking. This effect is defined as differential autogenous shrinkage, which adds to the drying moisture gradient. Internal self-desiccation and a discontinuous capillary pore-system are the fundamental properties of cement hydration. This renders any concrete, especially low water-cementitious-ratio (< 0.40) concrete, prone to warping.

Creep: Moisture shrinkage warping is a slow phenomenon in comparison to traffic loading. Since warping deformation is restrained by adjacent slabs, creep develops which reduces the slab uplift over time. This results in stress relaxation. To account for creep effects it is customary to use a lower E-modulus in stress analysis than the Young's modulus from strength testing. To account for creep effects, an effective modulus value of 2×10^6 psi is used in the analysis corresponding to approximately 50% of Young's modulus.

- The analysis results suggest that moisture warping from constant exposure to water of the slab bottom is a major factor, and that it alone can result in back-calculated TELTD values and associated permanent joint and corner uplift resulting in fatigue cracking.

- The findings support that a field surface profile of the slab edge will provide indications of the severity of slab uplift that can lead to top-down cracking. A profiling process can be used to develop new QC/QA specifications.

- The methodology presented herein was tested for a JPCP project that has developed premature transverse cracking. The TELTD range was obtained by matching the surface profile results with FE predictions using ISLAB 2000. Inspector daily reports were used to determine time of construction and field temperature information. They showed that construction in the east-bound direction occurred during cooler fall weather conditions, which precludes any significant built-in negative curl. Thus, it can be concluded that the cause of cracking is moisture shrinkage warping. These predictions were validated by a comprehensive field investigation project.

7.0 RECOMMENDATIONS

The recommendations from this study involve several areas and include needs for implementation.

- The results of this study suggest that poor subsurface drainage is the major cause for the permanent joint uplift condition found in the JPCP project example (I-96, CS 47065). There are possible design and construction issues related to the JPCP drainage system, such as type of drainage layers (dense-graded separator layer versus geotextile membrane) and location of the edge-drain, that need investigation. Portions of the subbase are becoming temporarily or permanently saturated along the slab-shoulder edge leading to pumping erosion and wetting of the slab surface, as water is not getting to the outlet drain trench soon enough.

- Slabs on stiff bases are more vulnerable to the effects from moisture warping and associated erosion. For example, if water becomes entrapped, unbonded overlays are prone to cracking from their reduced slab thickness (6 to 8 in.). The performance of these systems should be closely monitored.

- Maintaining a uniform temperature during summertime weather construction within a concrete cross section until time of set can eliminate or reduce the temperature component that contributes to permanent slab uplift. MDOT should initiate demo-projects with embedded wireless temperature sensors during paving to monitor the effectiveness of controlling adverse positive temperature gradients.

- MDOT should initiate new field test procedures for monitoring temperature development during paving and post construction surface elevation tests to monitor if slab uplift is an issue. A new laboratory beam test is proposed to determine influence of differential moisture shrinkage on concrete warping uplift.

IMPLEMENTATION OF STUDY FINDINGS

This research study achieved its objective of providing justification for the development of new acceptance criteria (specifications) to be used during construction for concrete pavement placement. Also, because the contractor's construction practices can have longer term ramifications affecting the concrete slab's condition, continued department monitoring of its condition after construction (contract) is completed is warranted.

The steps involved to implement the study's findings, after review and acceptance by the department, are similar to other past efforts to modify a specification, or when new requirements for construction are adopted. These steps are generally:

1. Education –Several new terms and concepts were introduced in this report. The department's affected technical staff will need some additional classroom explanation of these concepts to better understand their relationships to concrete pavement performance. Additional training and usage of the Finite Element Model,

ISLAB2000, is needed, which is essential for pavement analysis. The needed education and training could be conducted by the UM Pavement Center through an existing contract.

2. **Communication** - The department will need to explain the need for the additional acceptance criteria to the construction industry through their in-place committee contacts.

3. Preparation/Development - The department will need to draft and implement several new procedures, especially those involving quality control. These will include:

- A testing procedure, similar to UM's for beam uplift measuring the warping potential of various concrete mixtures.
- Temperature monitoring of the concrete slab during hot weather paving to determine its temperature gradient at time of set in order to calculate the extent and severity of built-in construction curl that may have occurred. Temperature monitoring should continue after construction to determine average daily temperature fluctuations through the slab.
- A procedure for determining the slab's surface profile to quantify any corner uplift and its duration. Monitoring should continue long term, as slab uplift caused by moisture warping only develops if subsurface water becomes trapped and remains in contact with the slab bottom.

4. **Introduction of new Test Procedures** - The department should select one or more pavement projects to implement and demonstrate the new specification requirements. The projects would provide the necessary adjustment time before the requirements are made permanent.

Summary- The department reintroduced JPCP in 1995 to improve the service life of concrete pavement by reducing the occurrence of transverse cracking, which over time becomes expensive to repair and negates the initial construction cost savings versus JRCP. The department is keenly aware that some JPCP projects since their construction developed premature mid-slab cracking. Several research studies have investigated why the cracking occurred, which results from a complex set of factors working interactively. This study emphasized a means to quantify risk impact for crack development from uplift.

The JPCP cracking phenomena is not completely understood, as learning will need to continue. Still, preventive measures to reduce the occurrence of cracks are known and should be implemented whenever possible. Implementation of preventive measures is not solely a department responsibility, as paving contractors have a decisive role in the solution through improved quality control and construction practices.

Thus, education and communication between the Department and Industry are essential. The following points should be emphasized:

- Agreement on the causes and solutions to prevent mid-slab cracking of JPCP.
- How to improve existing construction practices and quality control procedures to eliminate causes for cracking.
- Identify new QC/QA procedures that may be needed.

Because mid-slab cracking occurs after construction is completed, and the contract is completed, a warranty period is justified. The duration of the warranty and any financial assessment is a department matter.

8.0 REFERENCES

ASTM, "Estimating Concrete Strength by the Maturity Method, C1074-87," Annual Book of ASTM Standard, 1987

Beckemeyer, C. A., L. Khazanovich, H. Thomas Yu, "Determining Amount of Built-in Curling in Jointed Plain Concrete Pavement: Case Study of Pennsylnania I-80", Transportation Research Record 1809, pp 85-92, 2002

Beddoe, R., and Springenschmid, R., "Moisture Transport through Concrete Structural Components", (In German), Beton-und Stahlbetonbau 94 (4), pp. 158-166, 1999.

Eisenmann, J., and Leykauf, G., "Effect of Paving Temperatures on Pavement Performance.", *2nd International Workshop on the Design and Evaluation of Concrete Pavements*, Siguenza, Spain, pp. 419-431, 1990

ERES, "ISLAB2000 Finite Element Code for Rigid Pavement Analysis", ERES Consultants, Champaign, IL, Version 3.6. 2000, 1999

Franklin, R.E., "The Effect of Weather Conditions on Early Strains in Concrete Slabs", RRL Report No. LR266, Crowthorne, Berkshire, UK, 1969

Hansen, W., Wei, Y., Bennett, A., Smiley, D., "Warping of Jointed Plain Concrete Pavement from Inadequate Base Drainage", International Workshop on Best Practices for Concrete Pavements, Oct. 2007, Recife, Brazil.

Hansen, W., Smiley, D., Peng, Y., and Jensen, E.A., "Validating Top-Down Premature Transverse Slab Cracking in Jointed Plain Concrete Pavement (JPCP)," Transportation Research Record 1809, Transportation Research Board, Washington, D.C., 2002

Huang, Y. H, "Pavement Design and Analysis," Prentice Hall, 1993

Hatt, W. K., "Effect of Moisture on Concrete", Public Roads, Vol. 6, No. 1, March 1925

Janssen, D.J., "Moisture in Portland Cement Concrete", Transportation Research Record 1121, Transportation Research Board, Washington, D.C., 1987

Poblete, M. Garcia, A., David, J., Ceza, P., and Espinosa, R., "Moisture Effects on the Behavior of PCC Pavements", Proceedings, 2nd International Workshop on the Design and the Evaluation of Concrete Pavements, Siguenza, Spain, 1990

Powers, T.C., Copeland, L. E., and Mann, H.M, "Capillary Continuity or Discontinuity in Cement Paste", PCA Bull., 10, 2–12, 1959

Rao, S, Roesler, J.R., "Characterizing Effective Built-In Curling from Concrete Pavement Field Measurements", Journal of Transportation Engineering, ASCE, April , pp. 320-327, 2005

Rhodes, C.C., "Curing Concrete Pavements with Membranes", Michigan Department of Transportation, Research Report No. 145, 1950.

Springenschmid, R., Plannerer, M, "Experimental Research on the Test Methods for Surface Cracking of concrete", Institute for Building Materials, Technical University Munich, Germany, 2001

Suprenant, B., "Why Slabs Curl, Part I and II", Concrete International, American Concrete Institute, March and April, 2002

Yu, H.T., Khazanovich, L., Darter, M.I., and Ardani, A., "Analysis of Concrete Pavement Responses to Temperature and Wheel Loads Measured from Instrumented Slabs", Transportation Research Record, 1639, 1998

APPENDIX A: MEASUREMENTS OF CONCRETE COEFFICIENT OF THERMAL EXPANSION

A1. UM Test Method for Coefficient of Thermal Expansion of Concrete

1. Scope

1.1 This test method covers the determination of the coefficient of thermal expansion (CTE) of hydraulic cement concrete cores or cylinders. The specimens must be in a saturated condition.

2. Referenced Documents

2.1 AASHTO Standards:

TP60-00 Standard Test Method for the Coefficient of Thermal Expansion of Hydraulic Cement Concrete

3. Apparatus and Supplies

3.1 A concrete saw capable of sawing the ends of a cylindrical specimen perpendicular to the axis and parallel to each other.

3.2 Calipers suitable for measuring the specimen length to the nearest 0.004 in.

3.3 A temperature controlled water bath with a temperature range of 50°F to 122°F, capable of controlling the temperature to 0.18°F.

3.4 A rigid support frame for the specimen to be used during length change measurement. The frame should be designed to have minimal influence on the length change measurements obtained during the test, and support the specimen such that the specimen is allowed to freely adjust to any change in temperature.

3.5 Three submersible temperature-measuring devices with resolution of 0.18°F.

3.6 A reference concrete cylinder with a built-in thermal couple for measuring cylinder's temperature.

3.7 A submersible LVDT gage head with excitation source and digital readout, with a minimum resolution of 0.00001 in, and a range suitable for the test.

3.8 A computer-controlled data acquisition system capable of recording data continuously, with thermal couples connected to it.

3.9 A micrometer or other suitable device for calibrating the LVDT over the range to be used in the test.

4. Sample

4.1 Test specimens shall consist of 4-inch-diameter cores sampled from the concrete structure being evaluated, or 4-inch-diameter cylinders. The specimens shall be sawed perpendicular to the axis at a length of 7±0.08 inches. The standard reference material used for calibration shall be the same length as the test specimen so that the frame does not have to be adjusted between calibrations and testing. The sawed ends should be flat and parallel.

5. Procedure

5.1 The specimen shall be conditioned by submersion in saturated limewater at 73±4°F for not less than 48 hours.

5.2 Place the measuring apparatus, with LVDT attached, in the water bath and fill the bath with cold tap water. Place the three thermal couples in the bath at locations that will provide an average temperature for the bath as a whole.

5.3 Remove the specimen from the saturation tank and place the specimen in the measuring apparatus located in the controlled temperature bath, making sure that the lower end of the specimen is firmly seated against the support buttons, and that the LVDT tip is seated against the upper end of the specimen.

5.4 Place the reference concrete cylinder, with an embedded thermal couple, in the water bath for monitoring the temperature change in the tested specimen.

5.5 Set the temperature of the water bath to 50±2°F. When the bath reaches this temperature, allow the bath to remain at this temperature until thermal equilibrium of the specimen has been reached, as indicated by consistent readings of the LVDT to the nearest 0.00001inches taken for three consecutive ten minute periods. The recorded data are the initial readings.

5.6 Set the temperature of the water bath to 122±2°F. Once the bath has reached 122±2°F, allow the bath to remain at this temperature until thermal equilibrium of the specimen has been reached, as indicated by consistent readings of the LVDT to the nearest 0.00001 inches taken for three consecutive ten minute periods. The recorded data are the second readings.

5.7 Set the temperature of the water bath to 50±2°F. When the bath reaches this temperature, allow the bath to remain at this temperature until thermal equilibrium of the specimen has been reached, as indicated by consistent readings of the

LVDT to the nearest 0.00001 inches taken for three consecutive ten minute periods. The recorded data are the final reading.

6. Calculations

6.1 Calculate the Coefficient of Thermal Expansion, as follows:

$$CTE = \left(\Delta L_a / L_0 \right) / \Delta T \qquad \text{(A-1)}$$

Where:

ΔL_a = actual length change of specimen during temperature change

L_0 = measured length of specimen at room temperature

ΔT = measured temperature change

$$\Delta L_a = \Delta L_{measured} + \Delta L_{system} \qquad \text{(A-2)}$$

Where:

$\Delta L_{measured}$ = measured length change of specimen during temperature change

ΔL_{system} = length change of the supporting frame during temperature change

$$\Delta L_{system} = \alpha_{in\ var} \cdot \Delta T - \Delta L_{calibration} \qquad \text{(A-3)}$$

Where:

$\alpha_{in\ var}$ = CTE of invar used in the calibration run for determining the length change of the measuring apparatus

$\Delta L_{calibration}$ = measured length change of the 7-inch-long invar bar which is used in the calibration run. The calibration run follows the same procedure as the one in determining the CTE of specimen.

6.2 The test result is the average of the two CTE values obtained from the two test segments provided the two values are within $0.5 \times 10^{-6}/^{o}F$. If the two values are not within $0.5 \times 10^{-6}/^{o}F$ of each other, one or more additional test segments are completed until two successive test segments yield CTE values within $0.5 \times 10^{-6}/^{o}F$ of each other. The final CTE is the average of these two CTE values of each cylinder.

A2. Comparison between U of M and AASHTO TP60-00 Method

In the AASHTO TP60-00 test method, the specimen is heated in a water-bath from 50°F to 122°F, and then cooled down to 50°F. The lengths and temperatures of specimen at the points of 50°F and 122°F are recorded for CTE calculation for each segment. The CTE value of the test specimen is taken as the average of the heating and cooling segments, provided the two values are within 0.5 micro strain/°F. Apparently, there are a few limitations in the AASHTO TP60-00 method for these reasons:

- The actual curve of temperature versus length change is unknown within each segment: thus it is unclear whether thermal equilibrium is reached during the test.
- Only the water bath temperature is measured, which may not represent the concrete specimen's temperature.

Therefore, a few modifications were made at U of M based on AASHTO TP60-00 to provide a better control on the measurement accuracy. The modifications are as follows:

- The modified method measures the entire curve of temperature versus length change of specimen, and the CTE value is calculated using only the linear part of the temperature versus length change curve to achieve accuracy.
- A companion specimen, with a thermal couple embedded at the center, is submerged in the water bath for temperature monitoring. This temperature is taken as the temperature of the tested concrete specimen.
- Two specimens can be measured at the same time, which improves the efficiency.

The comparison of the AASHTO TP60-00 method and the U of M method is illustrated in Figure A-1. The entire CTE test setup at U of M is shown in Figure A-2.

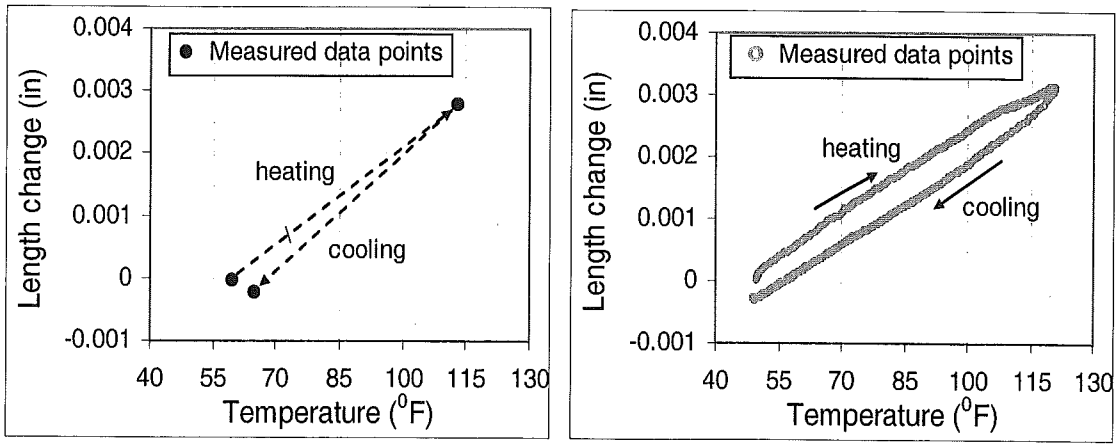

(a) AASHTO TP60-00 method (b) U of M method

Figure A-1
CTE test methods (AASHTO compared with U of M)

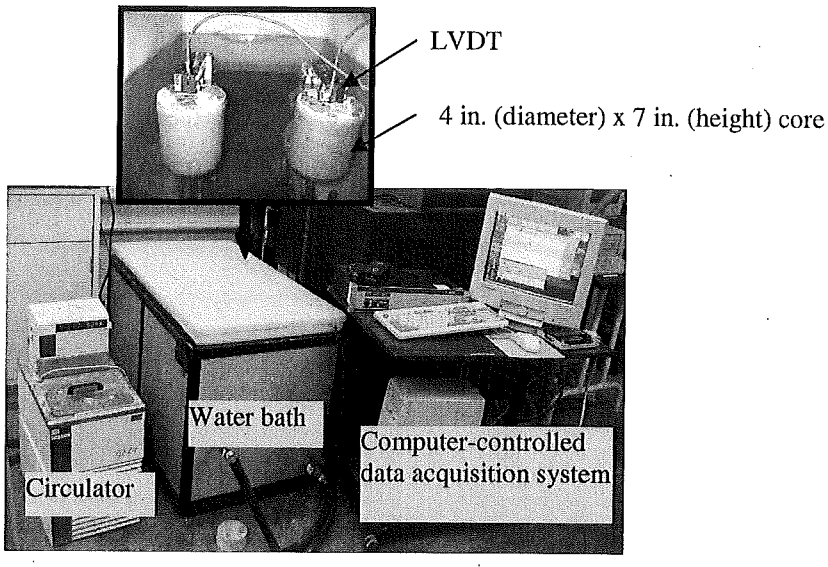

Figure A-2
CTE test setup at U of M

APPENDIX B: UM TEST METHOD FOR DETERMINING MOISTURE WARPING OF A CONCRETE BEAM

1. Scope

1.1 This test method covers the determination of the moisture warping of a concrete beam with drying at top and moisture wetting at bottom.

2. Referenced Documents

2.1 ASTM Standard
C 192 Practice for Making and Curing Concrete Test Specimens in the Laboratory

3. Apparatus and Supplies

3.1 The test is intended to simulate beam uplift from simultaneous drying from the top surface from evaporation and moisture wetting at the bottom, as shown in Figure B-1.

3.2 The concrete beam rests on a steel I-beam. The width and length of the steel I-beam should be slightly larger than the concrete beam. to allow a, tank to enclose the top of the steel beam to provide continual moisture to the concrete beam's bottom. One end of the concrete beam should be fixed to the steel I-beam through four bolts. The bolts can either be embedded in concrete beam or go through the pre-made holes in concrete beam and the steel I-beam.

3.3 A re-usable mold for making concrete beams.

3.4 A dial-gauge for measuring the beam uplift to the nearest 0.001 in.

3.5 An environmental chamber capable of controlling temperature to 0.18°F and relative humidity to 1%.

3.6 Water-proof paint to avoid moisture change between sealed concrete and environment.

4. Sample

4.1 Test specimen should be freshly cast into the mold.

4.2 Concrete specimen should be made according the ASTM C 192.

5. Procedure

5.1 After casting, the concrete beam should be sealed and cured in the environmental chamber at constant temperature.

5.2 The concrete beam can be de-molded after 7 days of curing after it has developed sufficient tensile strength.

5.3 A water-proofing paint is applied to the beam surfaces, except for the top and bottom, to ensure moisture exchange is controlled. The paint is applied in two layers. The second layer is applied only after the first layer has completely dried.

5.4 After painting, place concrete beam on the steel I-beam and bolt one end to the steel I-beam.

5.5 Add water to the built-in tank until the concrete beam bottom is in contact with water.

5.6 Attach dial-gauge to the free end of the concrete beam, zero the dial gauge and take a reading every 24 hours.

5.7 Continually check the water level during the entire testing period to ensure the beam bottom is always in contact with water.

6. Calculations

6.1 The uplift readings are plotted versus time.

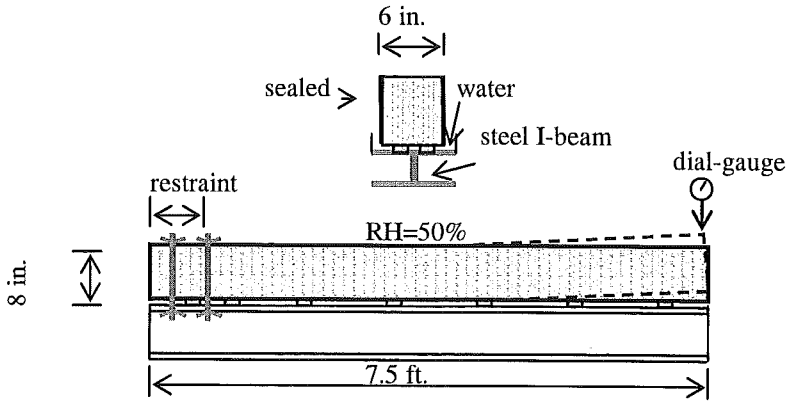

Figure B-1
Setup for beam warping test

It is recommended that MDOT incorporate the UM beam uplift test as a standard laboratory test for evaluating the effect of concrete material parameters on moisture

warping. Estimated material and machining cost for three steel molds shown in Figure 3-3 is approximately $5,000.

APPENDIX C: ANALYSIS OF SLABS WITH PARTIAL-DEPTH, FULL-WIDTH CRACKS

This study included software development by ERES Consultants for adding a fracture module for ISLAB 2000. This module determines the tendency of a partial depth crack (see Figure C-1) to become full-depth. The linear elastic fracture module used in ISLAB 2000 can predict the risk of full-depth cracking occurring when the stress intensity factor, k_1, exceeds the fracture toughness (the critical stress intensity factor), k_{1C}. The stress intensity factor is a function of crack depth, slab geometry, and the slab bending stress. The detailed calculation for k_1 is not introduced here. The facture toughness is a concrete property. It is determined in the laboratory by conducting a four-point bending test on a notched concrete beam.

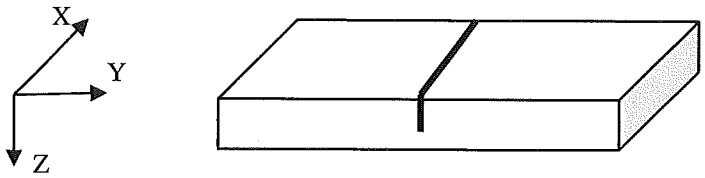

Figure C-1
Top-down, Partial-depth, full-width crack in a JPCP slab

Consider a JPCP project consisting of 6 consecutive slabs as shown in Figure C-2. Each slab is 12 ft. wide by 15 ft. long, resting on a base with a k-factor of 250 pci. The top-down, partial-depth, full-width cracks with an initial crack-to-depth ratio of 0.1 are located in the middle of each slab. The load transfer efficiency at all the joints is assumed to be 100 percent. Michigan 11-axle truck loading is applied at the critical position. In addition, the slabs are subjected to a TELTD value of -35°F.

For the slabs shown in Figure C-2, two slab thicknesses, 10 inches and 12 inches, were analyzed for the critical crack-to-depth ratio when sudden full-depth crack develops. Figure C-3 shows that the critical crack-to-depth ratios are 0.45 and 0.54 for the 10 in. and 12 in. slabs, respectively. Thus, the critical crack-to-depth ratio when sudden failure occurs depends on the slab thicknesses. A thicker slab can tolerate a larger crack-to-depth ratio before the slab is completely cracked.

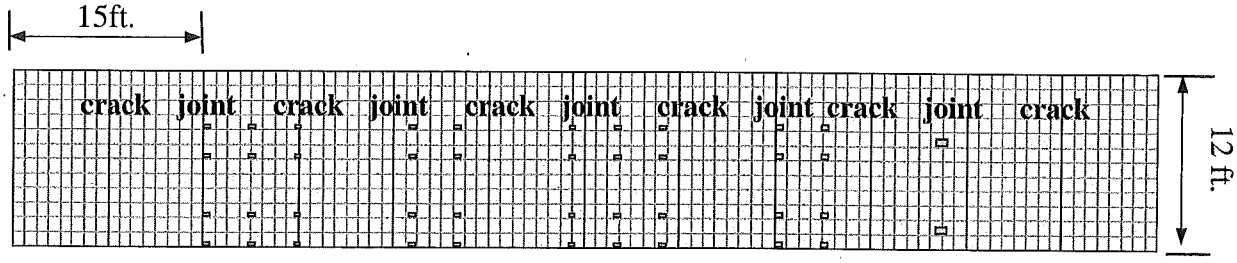

Figure C-2
Slab subjected to 11-axle truck loading, with top-down, partial-depth, full-width cracks located at mid-slab

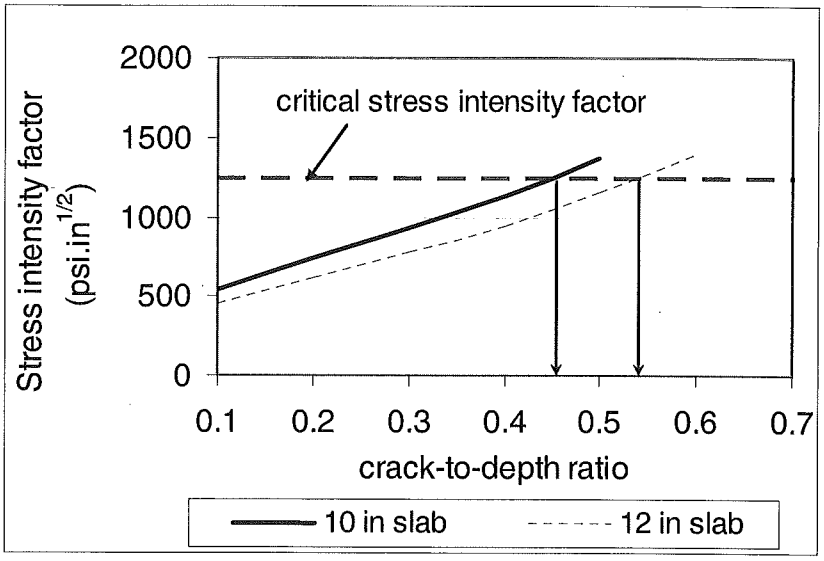

Figure C3
Critical crack-to-depth ratio when sudden full-depth cracking occurs for 10 in. and 12 in.-thick JPCP slab

APPENDIX D: DIPSTICK PROFILE MEASUREMENTS

The details of the field procedure used for slab surface profile measurements can be found in Appendix B of the "Distress Identification Manual for the Long-Term Pavement Performance Project", SHRP-P-338, pp. 127-137. This report with appendices can be downloaded from website: http://onlinepubs.trb.org/onlinepubs/shrp/SHRP-P-338.pdf

The estimated cost to MDOT for acquiring the Dipstick profiler, including operator training, is approximately $15,000.